USGS
science for a changing world

$^{40}Ar/^{39}Ar$ and K-Ar Geochronology and Tectonic Significance of the Upper Cretaceous Adel Mountain Volcanics and Spatially Associated Tertiary Igneous Rocks, Northwestern Montana

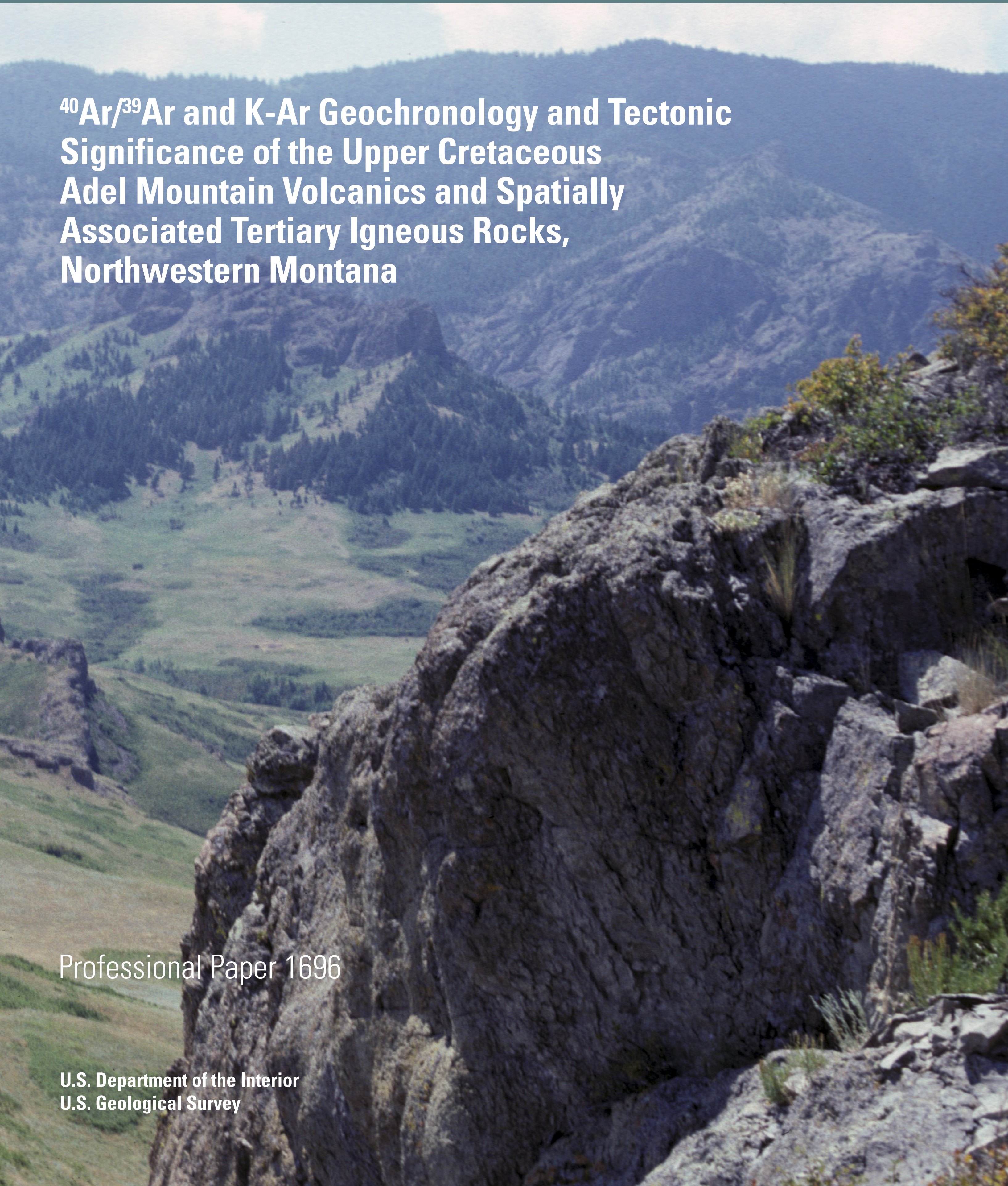

Professional Paper 1696

U.S. Department of the Interior
U.S. Geological Survey

$^{40}Ar/^{39}Ar$ and K-Ar Geochronology and Tectonic Significance of the Upper Cretaceous Adel Mountain Volcanics and Spatially Associated Tertiary Igneous Rocks, Northwestern Montana

By Stephen S. Harlan, Lawrence W. Snee, Mitchell W. Reynolds,
Harald H. Mehnert, R.G. Schmidt, Steve D. Sheriff, and Anthony J. Irving

Professional Paper 1696

U.S. Department of the Interior
U.S. Geological Survey

U.S. Department of the Interior
Gale A. Norton, Secretary

U.S. Geological Survey
Charles G. Groat, Director

U.S. Geological Survey, Reston, Virginia: 2005

For sale by U.S. Geological Survey, Information Services
Box 25286, Denver Federal Center
Denver, CO 80225

For more information about the USGS and its products:
Telephone: 1-888-ASK-USGS
World Wide Web: http://www.usgs.gov/

Contents

Figures

Tables

$^{40}Ar/^{39}Ar$ and K-Ar Geochronology and Tectonic Significance of the Upper Cretaceous Adel Mountain Volcanics and Spatially Associated Tertiary Igneous Rocks, Northwestern Montana

By Stephen S. Harlan,[1] Lawrence W. Snee,[2] Mitchell W. Reynolds,[2]
Harald H. Mehnert,[2] R.G. Schmidt,[3] Steve D. Sheriff,[4] and Anthony J. Irving[5]

Abstract

We report new $^{40}Ar/^{39}Ar$ and K-Ar dates from the Upper Cretaceous Adel Mountain Volcanics of northwestern Montana and spatially related Tertiary igneous rocks. The Adel Mountain volcanic field consists of about 900 square kilometers of lavas, associated volcaniclastic strata, and intrusions that lie astride the easternmost folds of the Montana disturbed belt of the Cordilleran fold and thrust belt. The Adel Mountain volcanic rocks have been intensely deformed by folds and thrust faults along their southwestern margin but are essentially undeformed to the east. Prior to isotopic dating, the age of the Adel Mountain Volcanics was the subject of debate, with age assignments ranging from Late Cretaceous to early Tertiary. Isotopic dates reported here demonstrate that the Adel Mountain Volcanics are clearly Late Cretaceous and that the volcanic rocks were probably emplaced during an approximately 2- to 3-million-year interval between about 76 to 73 mega-annum (Ma). The new dates from the Adel Mountain Volcanics are significant in that they provide a more refined and reliable age for the Late Cretaceous cratonic paleomagnetic reference pole for North America. The dates from the Adel Mountain Volcanics, as well as those from spatially related younger intrusions, also provide important constraints on the age of fold and thrust-belt deformation along the eastern margin of the Montana disturbed belt. Syntectonic deformation of the Adel Mountain Volcanics, as well as apparent folding and faulting of Tertiary quartz monzonite sills, indicates that contractional deformation clearly spanned the Late Cretaceous and may have extended to as young as the Paleocene/Eocene boundary at about 55.5 Ma. Elsewhere, posttectonic field relationships indicate that deformation may have ended prior to 60 Ma. Complexities in field relationships with respect to folds and faults shown by the early Tertiary intrusions as well as complications in the argon systematics indicate that these interpretations must be considered preliminary. Further field work and structural studies and additional high-precision geochronology are needed in order to place limits on the cessation of contractional deformation in this part of Montana. Unambiguously posttectonic dikes (47.5 Ma) that cut all deformed rocks and structures in the area indicate that disturbed belt deformation had clearly ceased by the early middle Eocene prior to the onset of widespread crustal extension in this part of the northern Cordillera.

Introduction

The Adel Mountain volcanic field of northwestern Montana consists of about 900 km^2 of lavas, associated volcaniclastic strata, and intrusions that lie astride the easternmost folds and thrust faults of the Montana disturbed belt segment of the Cordilleran fold and thrust belt (figs. 1, 2). The volcanic rocks of the field were first mapped and described by Lyons (1944). Subsequent informal usage by numerous investigators includes the names Adel Mountain volcanic field (Gunderson and Sheriff, 1991; Sheriff and Gunderson, 1990), the Adel Mountains volcanic field (Hyndman and Alt, 1987; Cunningham and Hyndman, 1999), or the Adel Mountain volcanic center (LaBranche, 1999). Maps and descriptions of the field and surrounding areas have been produced by Schmidt (1972a, 1972b, 1977, 1978), Soward (1975a, 1975b), Mudge and others (1982), Swenson (1988), and M.W. Reynolds (unpub. data, 1998). Descriptions of the petrology, petrogenesis and intrusions include Lyons (1944), Schmidt (1978), Beall (1972, 1973), Whiting (1977), Hyndman and Alt (1987); Irving and O'Brien (1994) and Cunningham and Hyndman (1999), whereas sedimentary characteristics of the volcaniclastic strata are described by LaBranche (1999).

[1]George Mason University, Fairfax, Virginia.
[2]U.S. Geological Survey, Denver, Colorado.
[3]U.S. Geological Survey, Reston, Virginia.
[4]Department of Geology, University of Montana, Missoula, Montana.
[5]Department of Geology, University of Washington, Seattle, Washington.

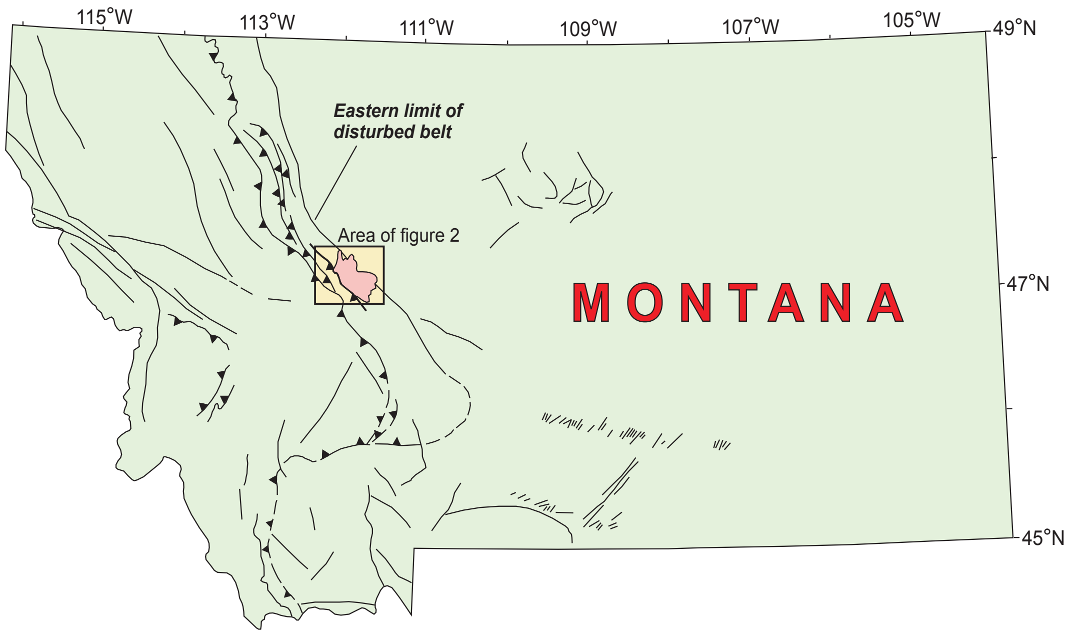

Figure 1. Generalized tectonic map of Montana showing major faults and the location of the Adel Mountain volcanic field (shaded) along the eastern margin of the Cordilleran fold and thrust belt. Also shown is the area of figure 2. Barbs on faults denote the upper plate of thrust faults.

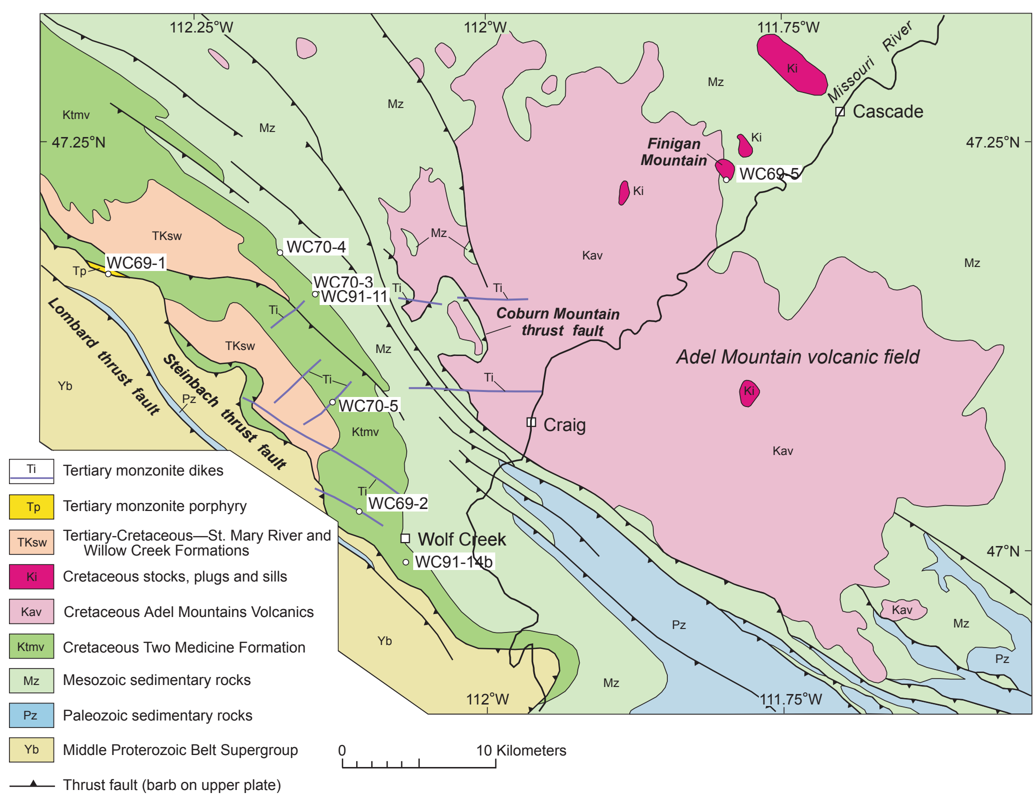

Figure 2. Simplified geologic map of northwestern Montana showing the location of the Adel Mountain volcanic field. Also shown are the locations of the some of the samples dated in this study. Unpublished map compilation of Schmidt (1968–73) with contributions from M.W. Reynolds for the southern part of the map area (unpublished mapping, 2002). Note that the Tertiary monzonite porphyry intrusion at sample location WC69-1 is shown as a sill that has been cut by the Steinbach thrust fault, although geologic mapping of Mudge and others (1982) suggests that this intrusion is a dike that cuts the thrust fault (see discussion in text on p. 14).

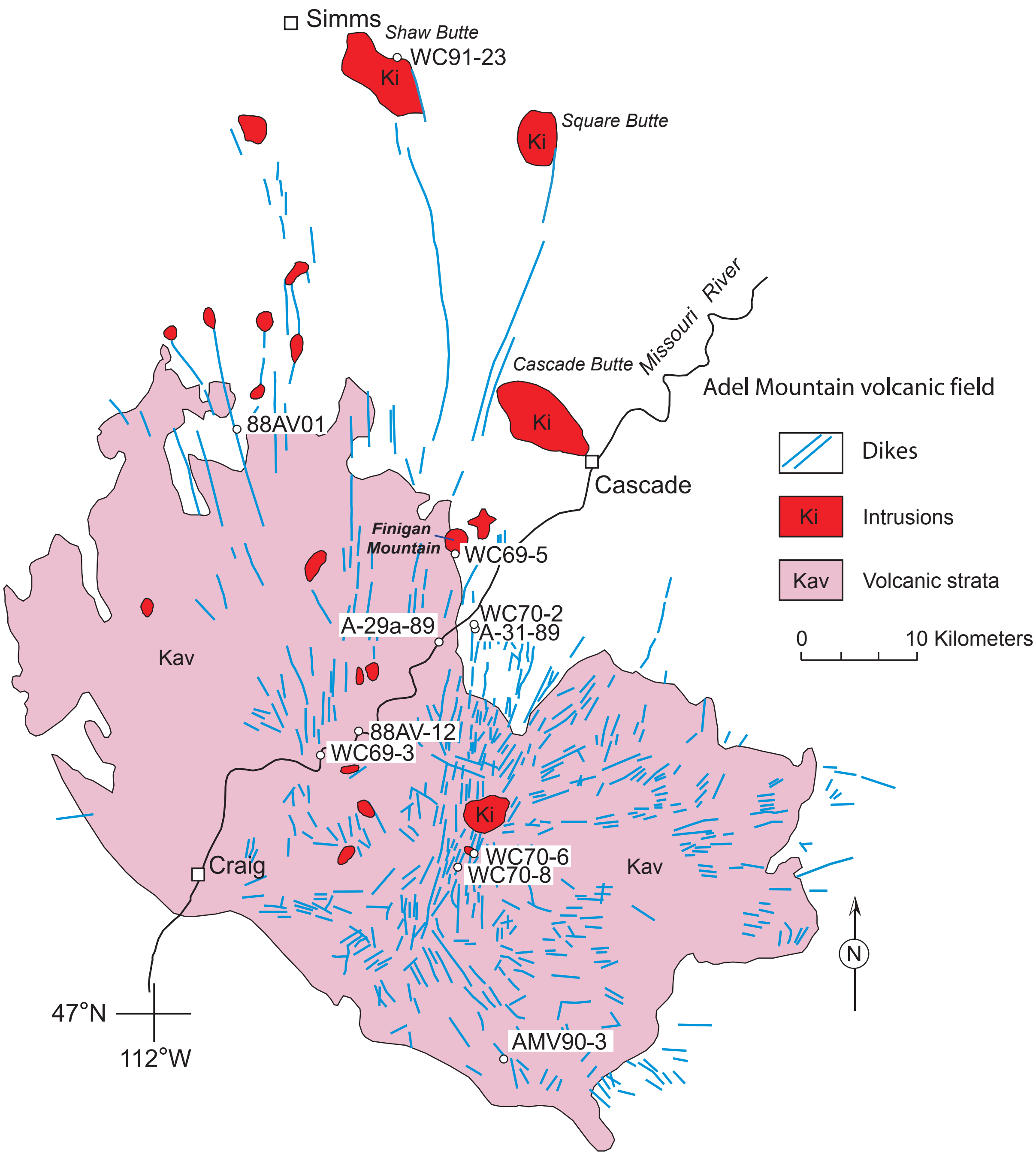

Figure 3. Simplified geologic map of the Adel Mountain volcanic field. Modified from Hyndman and Alt (1987) and Lyons (1944). Also shown are locations of samples from the Adel Mountain volcanic field and associated intrusive rocks dated in this study.

The volcanic field consists of about 1,000 m of potassium-rich clinopyroxene-phyric basalt and andesite (variously described as trachybasalt and trachyandesite). The field consists of lava flows, breccias, and volcaniclastic sediments that have been intruded by numerous plugs, sills, or other irregular bodies and by thousands of mafic dikes (fig. 3). Individual dikes range in thickness from a few centimeters to tens of meters. Most dikes are vertical to subvertical and crosscut the extrusive rocks (figs. 4*A*, 4*B*). Many of the dikes emanate radially or subradially from plugs or small stocks (figs. 3, 5). Several dikes also extend toward, and form feeders for, laccoliths located north and east of the main field (figs. 3, 6) (Beall, 1973; Whiting, 1977; Hyndman and Alt, 1987).

The volcanic rocks of the Adel Mountain field unconformably overlie sedimentary strata of the eastern facies of the Upper Cretaceous Two Medicine Formation along the western margin of the field (fig. 2) and to the east rest unconformably on Lower Cretaceous strata of the Kootenai and Lower and Upper(?) Cretaceous Blackleaf Formations (not shown). The unconformity in the southeastern part of the field spans a

Figure 4. Photographs of representative dikes from the Adel Mountain volcanic field. (*A*) Photograph of approximately 4-meter-thick subvertical shonkinite dike that cuts volcaniclastic strata of the Adel Mountain Volcanics. (*B*) Nearly vertical shonkinite dike that cuts Upper Cretaceous sedimentary strata east of the main part of the Adel Mountain volcanic field. The dike forms a pronounced topographic ridge and may be a feeder for one of the small laccoliths present east and northeast of the field.

stratigraphic thickness of about 1,219 m (Schmidt, 1978). This relation suggests uplift of this magnitude and erosion of the missing strata took place before the volcanic rocks of the Adel Mountain field were erupted (Schmidt, 1978). Along the eastern margin of the Cordilleran thrust belt at the southwestern margin of the field, the volcanic rocks have been moderately to intensely folded and cut by small imbricate thrust faults (fig. 2). Along the western margin of the field, the eastern facies of the Upper Cretaceous Two Medicine Formation were thrust eastward over the Adel Mountain Volcanics. To the south and southeast, some major thrust faults and large folds extend beneath and are overlapped by the volcanic rocks of the Adel Mountain field (fig. 2); this relation suggests that these structures predate eruption of the volcanic rocks. The observation that the volcanic rocks in some areas postdate folding and thrust faulting, but in other places are folded and cut by thrust faults, led Schmidt (1978) to suggest that the volcanic rocks of the Adel Mountain Volcanics are syntectonic with respect to the thin-skinned thrusting of the disturbed belt. Overall, the magnitude of contractile deformation in the field decreases to the east, and the volcanic strata, dikes, sills, and laccoliths north and east of the main field are essentially undeformed. The age of deformation represented by these folds and faults is generally regarded as Late Cretaceous to Paleocene, based on the ages of the youngest strata deformed.

Almost since the inception of geologic studies of rocks of the Adel Mountain volcanic field, their age has been a matter of controversy. Lyons (1944) initially suggested a Late Cretaceous age for these rocks based on the presence of plant fossils within a conglomerate near the exposed base of the volcanic rocks near Craig, Montana. Similarly, Chadwick (1972) considered them to be Late Cretaceous in age. Recent detailed geologic mapping along the southeast edge of the volcanic field also suggests a Late Cretaceous age for the rocks (M.W. Reynolds, unpub. data, 1998). In contrast, Schmidt (1978) suggested that the Adel Mountain Volcanics were likely of early Paleocene age based on structural and stratigraphic arguments. He also noted the compositional similarity of the Adel Mountain volcanic rocks to Paleocene and Eocene alkaline rocks of the central Montana alkalic province exposed east of the Adel Mountain volcanic field and to rocks of the Eocene Absaroka Volcanic Supergroup exposed to the southeast. Geologic mapping by Mudge and others (1982) also assigned them an uncertain Paleocene age.

In order to resolve the age of the volcanic rocks of the Adel Mountain field, a suite of samples was collected for isotopic dating by R.G. Schmidt and H.H. Mehnert in 1969 and 1970, as part of ongoing U.S. Geological Survey geologic investigations of this part of Montana. These samples were dated in the early 1970s, but neither the dates nor the sample locations were formally published. However, a March 1984 copy of the U.S. Geological Survey's Geologic Division internal newsletter ("The Cross Section") noted that Mehnert and Cebula had obtained K-Ar dates of 75±2.3 Ma and 72.9±2.1 Ma (error on dates at $\pm 2\sigma$) on hornblende and biotite from samples of trachybasalt and monzonite from the Adel Mountain Volcanics. Reportedly, these samples were collected from the lower breccia of Lyons (1944) near Wolf Creek, Montana, and were considered to represent the base of the Adel Mountain Volcanics. Thus, these dates clearly demonstrated that the lower part of the Adel Mountain Volcanics is Late Cretaceous in age.

Confusion regarding the provenance of these samples was inadvertently introduced by Sheriff and Gunderson (1990) and Gunderson and Sheriff (1991) who suggested that the samples credited to Mehnert and Cebula in the Geologic Division newsletter were not from the Adel Mountain Volcanics but rather were part of the structurally and stratigraphically lower Upper Cretaceous Two Medicine Formation. As part of a paleomagnetic investigation of the Adel Mountain Volcanics, Sheriff and Gunderson (1990) and Gunderson and Sheriff (1991) published two commercially obtained K-Ar dates from the Adel Mountain Volcanics, which are also consistent with a Late Cretaceous age. One whole rock sample obtained from a flow "deep within the volcanic pile" gave an apparent age of 81.1±3.5 Ma, whereas biotite from one of the shonkinite dikes that crosscut the volcanic rocks gave an age of 71.2±2.7 Ma (errors on both dates at ±1σ). Thus, Sheriff and Gunderson (1990) and Gunderson and Sheriff (1991) suggested that volcanism in the Adel Mountain volcanic field spanned an approximately 10-m.y. interval from 81 to 71 Ma; from these dates they assigned an arithmetic mean of 76 Ma for their paleomagnetic pole from the Adel Mountain Volcanics. This age and pole are significant as this pole is considered to be one of the only valid reference poles for cratonic North America during a critical episode of rapid apparent polar wander for the mid-Cretaceous to Tertiary segment of the North American apparent polar wander path within normal polarity Chron 33.

K-Ar dates from volcanic rocks along the southeastern part of the Adel Mountain volcanic field were reported by Bellon and others (1989). They reported nine dates with apparent ages ranging from 74.2 to 60.4 Ma. Unfortunately, the locations and descriptions of rocks dated are poorly documented; thus, the geologic significance and accuracy of these K-Ar dates are impossible to evaluate.

In this paper, we report sample locations, sample descriptions, K-Ar dates, and analytical data for the original samples collected by R.G. Schmidt and H.H. Mehnert in 1969 and 1970. These samples include those from the Adel Mountain Volcanics, as well as other spatially related Tertiary igneous rocks important to the geologic evolution of this area. In order to further constrain the age of the Adel Mountain Volcanics, we reanalyzed the original mineral separates of Schmidt and Mehnert by using the high-precision $^{40}Ar/^{39}Ar$ incremental step-heating method. In addition, we reanalyzed, using the $^{40}Ar/^{39}Ar$ method, the original whole rock and biotite samples dated by Sheriff and Gunderson (1990) as part of their paleomagnetic study, and we report new $^{40}Ar/^{39}Ar$ dates for additional samples, most of which were collected during 1989 and 1991. These new isotopic dates contribute to an enhanced understanding of the age of the Adel Mountain volcanic field and associated paleomagnetic pole and contribute to an improved understanding of the volcanic rocks and their place in the structural, tectonic, and magmatic evolution of the northern Rocky Mountains.

Acknowledgments

Ross Yeoman of the U.S. Geological Survey provided valuable laboratory assistance during the course of this study. Jerry Cebula prepared many of the mineral separates used in this study. Edward du Bray, Karl Kellogg, and Lori E. Apodaca provided constructive and useful reviews of the manuscript.

Analytical Methods

Seventeen mineral and one whole rock sample were collected from volcanic and intrusive rocks at 13 localities in the Adel Mountain volcanic field and surrounding areas for K-Ar and (or) $^{40}Ar/^{39}Ar$ dating. Sample descriptions and locations are given in the Appendix, and the locations are shown in figures 2 and 3. Whole rock and mineral separates were prepared by standard crushing and sieving techniques. Mineral concentrates were prepared using standard gravimetric (heavy liquid) and magnetic separation techniques. Samples analyzed by the $^{40}Ar/^{39}Ar$ method were handpicked to an estimated visual purity of greater than 99.9 percent. Whole rock and amphibole separates were washed in dilute hydrochloric or nitric acid to remove any carbonate alteration.

Potassium analyses for potassium-argon dating were performed by E.H. Brandt using a lithium metaborate flux fusion-flame photometry method (Ingamells, 1970). Argon extraction and purification techniques used in this study are similar to those described by Dalrymple and Lanphere (1969). Argon isotopes were analyzed by using standard isotope dilution procedures using a 60°-sector, 15.2-cm-radius, Nier-type mass spectrometer operated in the static mode. The estimated analytical uncertainty for the calculated potassium-argon age is reported as ±2σ. A summary of the potassium-argon (K-Ar)

Figure 5. View southwest along U.S. Interstate 15 showing the north margin of the Twin Sisters stock and the numerous mafic dikes that emanate radially from this intrusion. The dikes commonly are resistant to erosion and form prominent linear ridges.

Figure 6. Square Butte laccolith east of the Adel Mountain volcanic field. (*A*), View showing gently dipping Upper Cretaceous sedimentary rocks exposed near base of Square Butte laccolith. Note the prominent columnar jointing present in the intrusion. (*B*), View northwest showing prominent subhorizontal jointing shown in the Square Butte laccolith intrusion.

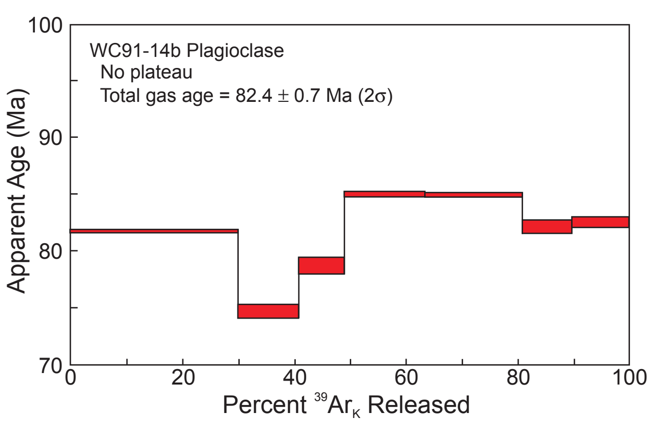

Figure 7. $^{40}Ar/^{39}Ar$ age spectrum for a plagioclase concentrate from a crystal vitric tuff from the volcanic member of the western facies of the Upper Cretaceous Two Medicine Formation. The analytical error in the apparent age for each temperature step in the age spectrum is represented by the height of the shaded rectangle; the proportion of $^{39}Ar_K$ released in the incremental heating experiment is represented by the length of the shaded rectangle.

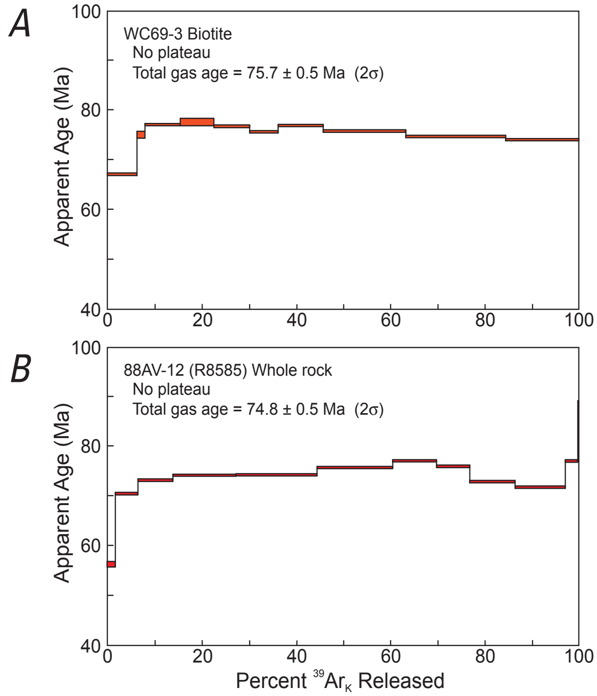

Figure 8. $^{40}Ar/^{39}Ar$ age spectra for (*A*), a biotite concentrate and (*B*), a whole rock sample from flows near the base of the Adel Mountain Volcanics. The analytical error in the apparent age for each temperature step in the age spectrum is represented by the height of the shaded rectangle; the proportion of $^{39}Ar_K$ released in the incremental heating experiment is represented by the length of the shaded rectangle.

ages and related analytical data is reported in table 1; detailed analytical data for samples dated by the K-Ar method are given in table A1.

Whole rock and mineral separates for $^{40}Ar/^{39}Ar$ dating were loaded in aluminum foil capsules, sealed in silica vials, and irradiated for 30 hours in the central thimble of the U.S. Geological Survey (USGS) TRIGA reactor in Denver, Colorado. Vertical and horizontal gradients in neutron fluence in the irradiated package were monitored by 8 to 10 standards distributed along the length of each vial; the geometry of the irradiated package was such that each unknown sample was adjacent to at least one standard. Neutron fluence was monitored using hornblende standard MMhb-1 (Samson and Alexander, 1987), which has a K-Ar age of 523.1±2.6 Ma (Renne and others, 1998). Corrections for reactor-produced interfering reactions were made using argon isotopes of K_2SO_4 and CaF_2 irradiated in each package.

After irradiation, the samples were progressively degassed in a double-vacuum resistance furnace in a series of eight to ten 20-minute-long steps to a maximum temperature of 1,450°C. After each heating step, the gas was collected and purified using Zr-Al-Ti getters, and all five argon isotopes were measured using a mass spectrometer operated in the static mode. Apparent ages were calculated using decay constants recommended by Steiger and Jäger (1977). Argon data were evaluated using age spectra, apparent $^{39}Ar/^{37}Ar$ ratios (for whole rock and hornblende samples), and $^{39}Ar/^{40}Ar$

Table 1. Summary of isotopic dating results from the Adel Mountain Volcanics and spatially associated volcanic and intrusive rocks, north-central Montana.

[P, plagioclase; B, biotite; WR, whole rock; H, hornblende; Tg, total gas; Tp, plateau date; --, not applicable; <, less than. The preferred age is our best estimate of the geologic age of the sample based on our interpretation of the results of the isotopic dating. Analytical error associated with isotopic ages given at ±2σ]

Sample number	Stratigraphic unit	Rock type	Material dated	K-Ar date (Ma)	$^{40}Ar/^{39}Ar$ date (Ma)	Preferred age (Ma)
Rocks that predate Adel Mountain Volcanics						
WC91–14b	Unit C, Western Volcanic Member, Two Medicine Formation	Crystal-vitric ash-flow tuff	P	--	Tg = 82.4±0.7	--
Adel Mountain Volcanics and related intrusive rocks						
WC69–3	Adel Mountain Volcanics	Augite-biotite trachybasalt breccia	B	73.2±2.1	Tg = 75.7±0.5	75.7±0.5
88AV–12	Adel Mountain Volcanics	Aphyric “shonkinite” flow	WR	[1]81.1±7.0	Tg = 74.8±0.5	74.8±0.5
A-29a–89	Adel Mountain Volcanics dike	Hornblendite xenolith in trachyandesite dike	H	--	Tp = 74.74±0.42	74.74±0.42
A-31–89	Adel Mountain Volcanics dike	Sanidine-phyric microsyenite dike	H	--	Tp = 73.17±0.42	73.17±0.42
WC70–2	Adel Mountain Volcanics dike	Hornblende-biotite monzonite dike	H	75.0±2.3	Tp = 73.90±0.40	73.90±0.40
			B	72.9±2.1	Tg = 73.9±0.7	--
AMV90–3	Adel Mountain Volcanics dike	Biotite-bearing trachybasalt dike	B	--	Tg = 74.2±0.6	74.2±0.6
WC70–8	Adel Mountain Volcanics dike	Biotite-bearing trachybasalt dike	B	73.7±2.1	Tp = 73.72±0.62	73.72±0.62
WC70–6	Intrusion cutting Adel Mountain Volcanics	Biotite monzonite	B	74.0±2.1	Tp = 74.67±0.42	74.67±0.42
88AV01	Adel Mountain Volcanics dike	Biotite “shonkinite”	B	[1]71.2±5.4	Tg = 73.4±0.4	--
WC91–23	Shaw Butte laccolith	Biotite (potassic) monzonite	B	--	Tp = 73.68±0.40	73.68±0.40
WC69–5	Intrusion that may cut Adel Mountain Volcanics? (relationship uncertain)	Hornblende monzonite	H	83.3±2.5	Tg = 81.2±0.5	<75.9
Tertiary intrusive rocks						
WC69–1	Sill apparently cut by Steinbach thrust	Biotite-bearing quartz monzonite porphyry	B	[2]59.6±1.6	--	59.6±1.6
WC70–3	Sill intruding lower part of western facies of Two Medicine Formation	Biotite-bearing monzonite porphyry	B	55.8±1.4	Tg = 56.8±0.3	56.8±0.3
WC91–11	Sill intruding lower part of western facies of Two Medicine Formation	Biotite-bearing monzonite porphyry	B	--	Tg = 56.2±0.3	56.2±0.3
WC70–4	Sill intruding western facies of Two Medicine Formation and cut by thrust fault	Biotite-hornblende quartz monzonite porphyry	H	64.8±1.6	Tg = 60.7±0.4	--
			B	54.9±1.6	Tg = 52.1±0.6	--
WC70–5	Dike intruding volcanic member of western facies of Two Medicine Formation	Hornblende monzonite	H	50.4±1.2	Tp = 47.48±0.30	47.21±0.30
WC69–2	Dike intruding volcanic member of western facies of Two Medicine Formation	Hornblende monzonite	H	47.5±1.3	Tp = 47.55±0.48	47.55±0.48

[1]Originally reported by Sheriff and Gunderson (1990).

[2]Although the K-Ar date is reported here, no $^{40}Ar/^{39}Ar$ analysis was performed as the original separate could not be found. This date has been noted in several reports including Schmidt (1978) and Whipple and others (1987), but neither the analytical data nor sample descriptions have previously been reported.

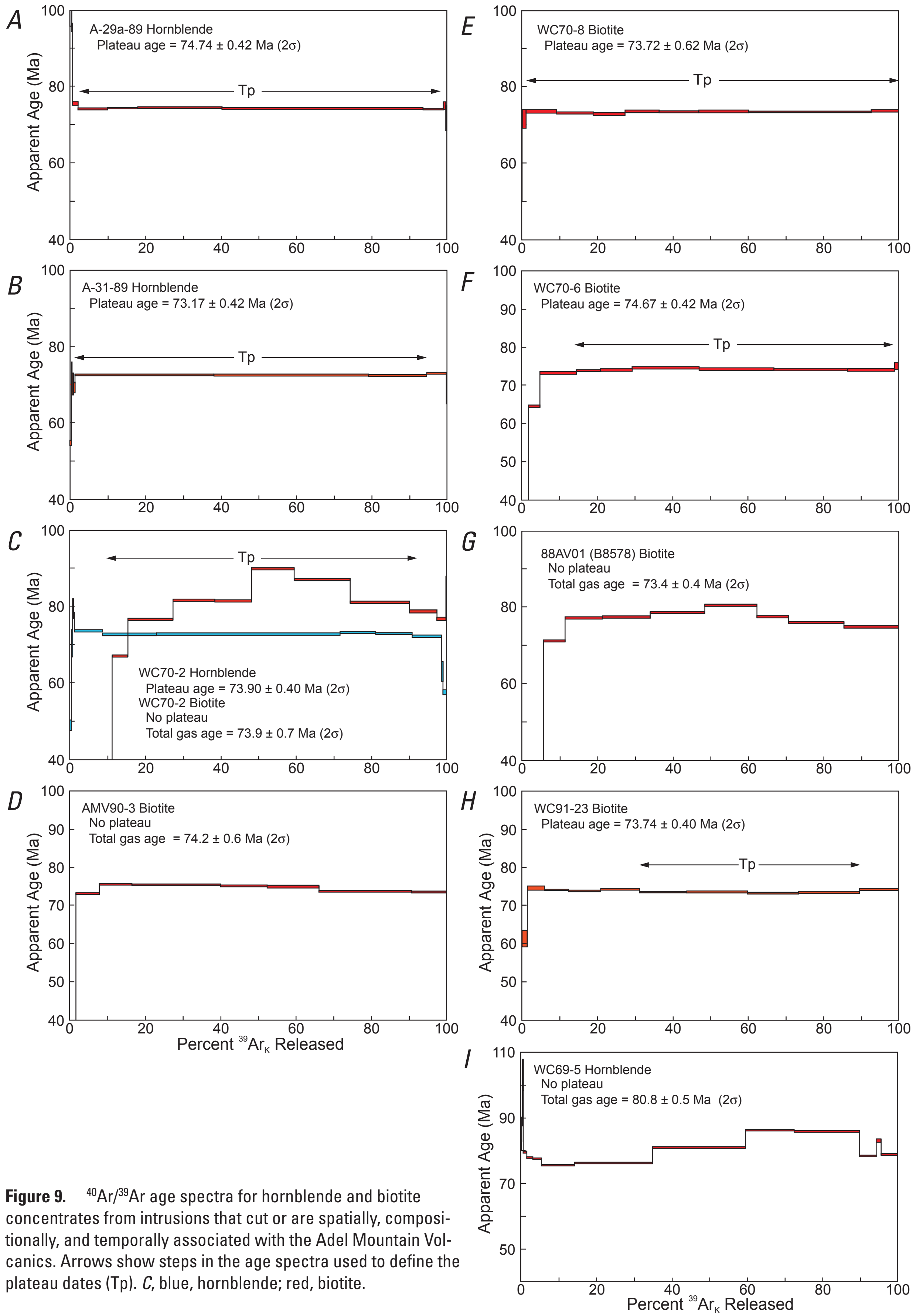

Figure 9. $^{40}Ar/^{39}Ar$ age spectra for hornblende and biotite concentrates from intrusions that cut or are spatially, compositionally, and temporally associated with the Adel Mountain Volcanics. Arrows show steps in the age spectra used to define the plateau dates (Tp). *C*, blue, hornblende; red, biotite.

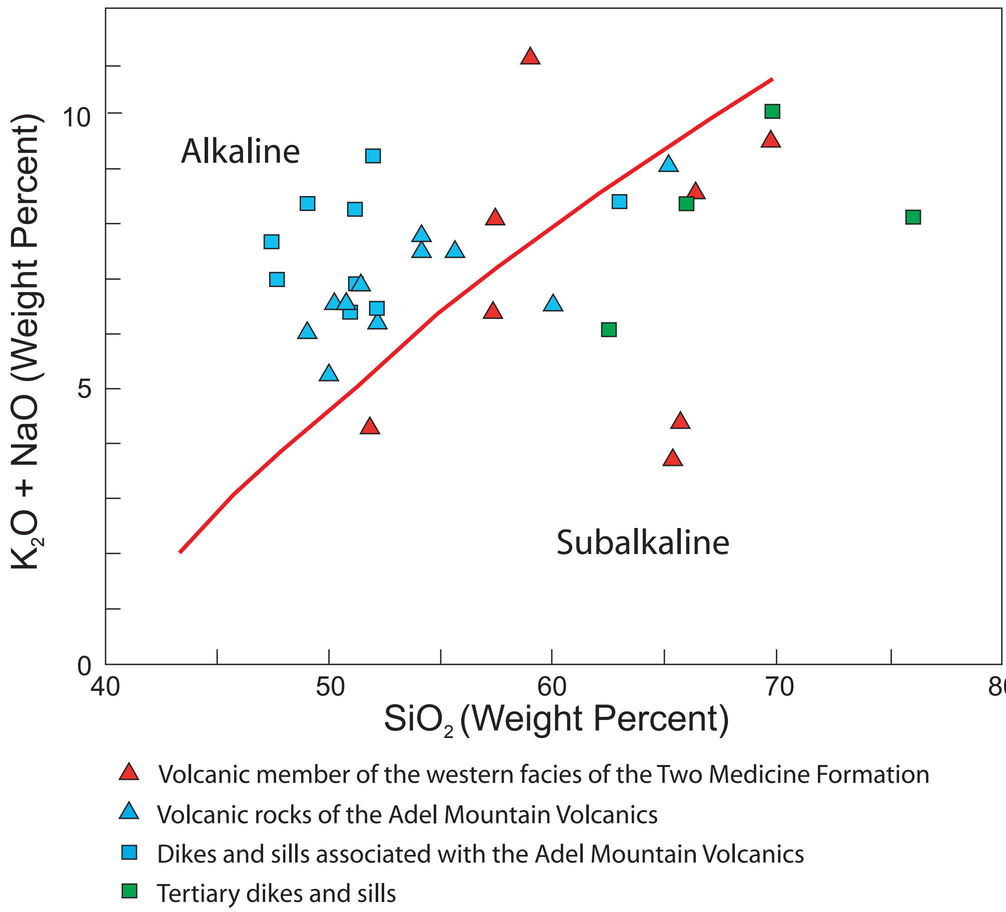

Figure 10. Variation diagram showing the abundance of alkali vs. silica for samples from the volcanic member of the western facies of the Upper Cretaceous Two Medicine Formation, the Upper Cretaceous Adel Mountain Volcanics, and Tertiary dikes and sills. The solid line separates the alkaline and subalkaline fields using the Irvine and Baragar (1971) classification scheme. Sources for the geochemical data are Lyons (1944), Beall (1973), Soward (1975a), and Schmidt (1978).

versus $^{36}Ar/^{40}Ar$ correlation diagrams. The determination of whether the individual apparent ages in an age spectrum yielded a “plateau” was made using the criteria of Fleck and others (1977). Following these criteria, a plateau is defined as comprising two or more contiguous gas fractions that yield apparent ages statistically indistinguishable at the 95-percent confidence level (using the critical value test of McIntyre, 1963, as applied by Dalrymple and Lanphere, 1969) and which together constitute greater than 50 percent of the total potassium-derived ^{39}Ar ($^{39}Ar_K$) released in the incremental heating experiment. Plateau ages were calculated using a weighted mean based on the proportion of $^{39}Ar_K$ released during the incremental heating experiment. Total gas, plateau, and correlation ages are given at $\pm 2\sigma$ and include the analytical uncertainty in the determination of the fluence parameter J. A summary of the results of the $^{40}Ar/^{39}Ar$ incremental heating experiments is listed in table 1 along with our preferred ages based on interpretation of the isotopic analyses. Individual age spectra are shown in figures 7 to 10. Total gas, plateau, and preferred ages, as described in the text, are listed in table 1; detailed $^{40}Ar/^{39}Ar$ analytical data for individual samples are listed in table A2. Complete details on procedures used in the USGS, Denver Argon Geochronology Laboratory are available in Snee (2002).

Results and Interpretation

Upper Cretaceous Two Medicine Formation

Sample WC91-14b (fig. 2) was collected from a crystal vitric tuff in unit C of the volcanic member of the western facies of the Upper Cretaceous Two Medicine Formation (Schmidt, 1978) exposed in a quarry approximately 1.6 km south of Wolf Creek, Montana (fig. 2). The sample contains plagioclase and biotite as phenocrysts, and both were separated for $^{40}Ar/^{39}Ar$ dating. Unfortunately, X-ray diffraction analysis and visual examination indicated that the biotite was heavily chloritized, and the biotite concentrate was deemed inappropriate for further analysis. Because the plagioclase concentrate visually appeared unaltered, the plagioclase was irradiated and dated by the ^{40}Ar/^{39}Ar method. The plagioclase gave a total gas age of 82.4±0.7 Ma (2σ) and a discordant age spectrum (fig. 7). Because of the discordant age spectrum, the geologic age of this sample is difficult to assess with certainty. The total-gas age for the sample, however, is similar to single-crystal, ^{40}Ar/^{39}Ar total fusion plagioclase and biotite dates of 80 to 74 Ma reported for bentonites and a crystal-rich tuff intercalated with nonmarine Two Medicine Formation strata elsewhere in northwestern Montana (Rogers and others, 1993). Given complications inherent in the plagioclase age spectrum reported here, we suggest that the ^{40}Ar/^{39}Ar dates based on the plagioclase total fusion analyses of Rogers and others (1993) probably should be interpreted with some caution.

Adel Mountain Volcanics and Associated Intrusions

Two samples were collected and dated from volcanic rocks interpreted to be at or near the base of the Adel Mountain Volcanics. Because the rocks dated are at or near the base of the volcanic pile, they potentially provide a means of dating the approximate age of the onset of Adel Mountain volcanism. Sample WC69-3 is a biotite concentrate from a clast in a coarse volcanic breccia (fig. 3) collected by R.G. Schmidt. The second sample (88AV-12) is the whole rock sample collected by Gunderson and Sheriff (1991) and described as being from deep within the Adel Mountain volcanic pile (fig. 3). The conventional K-Ar date obtained by Gunderson and Sheriff (1991) is 81.1±3.5 Ma (1σ).

Sample WC69-3 gave a conventional K-Ar apparent age of 73.2±2.1 Ma (2σ) (table 1). ^{40}Ar/^{39}Ar analysis of the same mineral concentrate gave a discordant age spectrum with no plateau and a total gas age of 75.7±0.5 Ma (2σ) (fig. 8*A*). The overall hump-shaped spectrum is indicative of biotite samples that have experienced some degree of chloritization (for example, Lo and Onstott, 1989). The interpretation of such spectra is complex, but the best estimate of the age of such samples is probably given by their total gas age.

The high-potassium whole rock sample of Sheriff and Gunderson (1990) and Gunderson and Sheriff (1991), sample 88AV-12, also gave a complex, hump-shaped age spectrum (fig. 8*B*) with an apparent total gas age of 74.8±0.5 Ma (2σ), which is significantly younger than the conventional whole rock date of 81.1±3.5 Ma (1σ). Again, the best estimate of the age of this sample is given by the ^{40}Ar/^{39}Ar total gas age of 74.8±0.5 Ma. Together, these two dates from near the base of the Adel Mountain volcanic pile suggest that Adel Mountain volcanic activity began about 76 to 75 Ma. A more precise estimate of the age of the initiation of volcanism is not warranted given the overall discordant nature of the ^{40}Ar/^{39}Ar age spectra of these two samples.

Ten mineral separates from nine intrusions associated with the Adel Mountain Volcanics were dated using conventional K-Ar and(or) ^{40}Ar/^{39}Ar methods (tables 1, 2; figs. 9*A*–*I*). Most of the intrusions from which the samples are derived are dikes or small stocks or plugs that cut the Adel Mountain Volcanics. One sample (WC91-23) was also collected from the Shaw Butte laccolith (fig. 3) about 25 km north of the field, which is thought to be temporally associated with the Adel Mountain Volcanics (Hyndman and Alt, 1987).

Hornblende and biotite concentrates separated from six samples from intrusive rocks, including the sample from the Shaw Butte laccolith, gave internally consistent ages throughout most of the step-heating experiment that satisfy the rigid plateau criteria of Fleck and others (1977). Hornblende and biotite concentrates from these samples give dates that range from 74.74 to 73.17 Ma (table 1; fig. 9). Three biotite samples from dikes yield mildly to strongly discordant age spectra with total gas ages ranging from 74.2 to 73.4 Ma, an age range which is within the distribution of plateau dates from the well-behaved samples previously described. Two samples that yield well-behaved age spectra and plateau dates are from an igneous-textured hornblende xenolith in a felsic microsyenite (A-31-89) dike and primary igneous hornblende from a monzonite (WC70-2) dike. These dikes are part of a swarm of dikes considered by Schmidt (1978) to be among the youngest igneous phases associated with the Adel Mountain Volcanics. These samples yield apparent ages of 73.17 Ma and 73.90 Ma, respectively (figs. 9*B* and 9*C*). These dates effectively represent the age that Adel Mountain volcanic activity ended. The geochronologic data reported here suggest that the bulk of the Adel Mountain volcanic rocks may have been emplaced in as little as 2 to 3 m.y.

^{40}Ar/^{39}Ar dates from the Adel Mountain Volcanics flows and the crosscutting dikes and stocks indicate that the bulk of Adel Mountain volcanism occurred between about 76 to 73 Ma. The only qualification to this proposed 3-m.y. age span for Adel Mountain volcanism comes from K-Ar and isotopic dates from a hornblende monzonite stock exposed at Finigan Mountain along the eastern margin of the Adel Mountain Volcanics (fig. 2; sample location WC69-5, fig. 3) (Soward, 1975b). This sample gave a K-Ar date of 83.3±2.5 Ma, significantly older than the proposed age range for the Adel Mountain Volcanics. Similarly, ^{40}Ar/^{39}Ar analysis yielded a total gas date of 81.2±0.5 Ma (table 1) and a strongly discordant, somewhat U-shaped age spectrum (fig. 9*I*) suggestive of incorporation of excess ^{40}Ar. The lowest age in the U-shaped part of spectra of this type is commonly interpreted to represent a maximum age for the sample, in this case, about 75.9 Ma. This age is slightly older than the age range established by the other samples but may not be inconsistent if it indeed represents a maximum age for the sample. Alternatively, the monzonite at Finigan Mountain may not be part of the Adel Mountain Volcanics. It could represent an outlier of intrusive rocks associated with the 80- to 74-Ma volcanic member of the western facies of the Two Medicine Formation that intruded its own extrusive carapace. Indeed, evidence for an extrusive origin for this feature includes the presence of small areas of vent breccia and probable extrusive breccia (Soward, 1975b). If the Finigan Mountain monzonite is part of the volcanic member of the western facies of the Two Medicine Formation, then the contact between

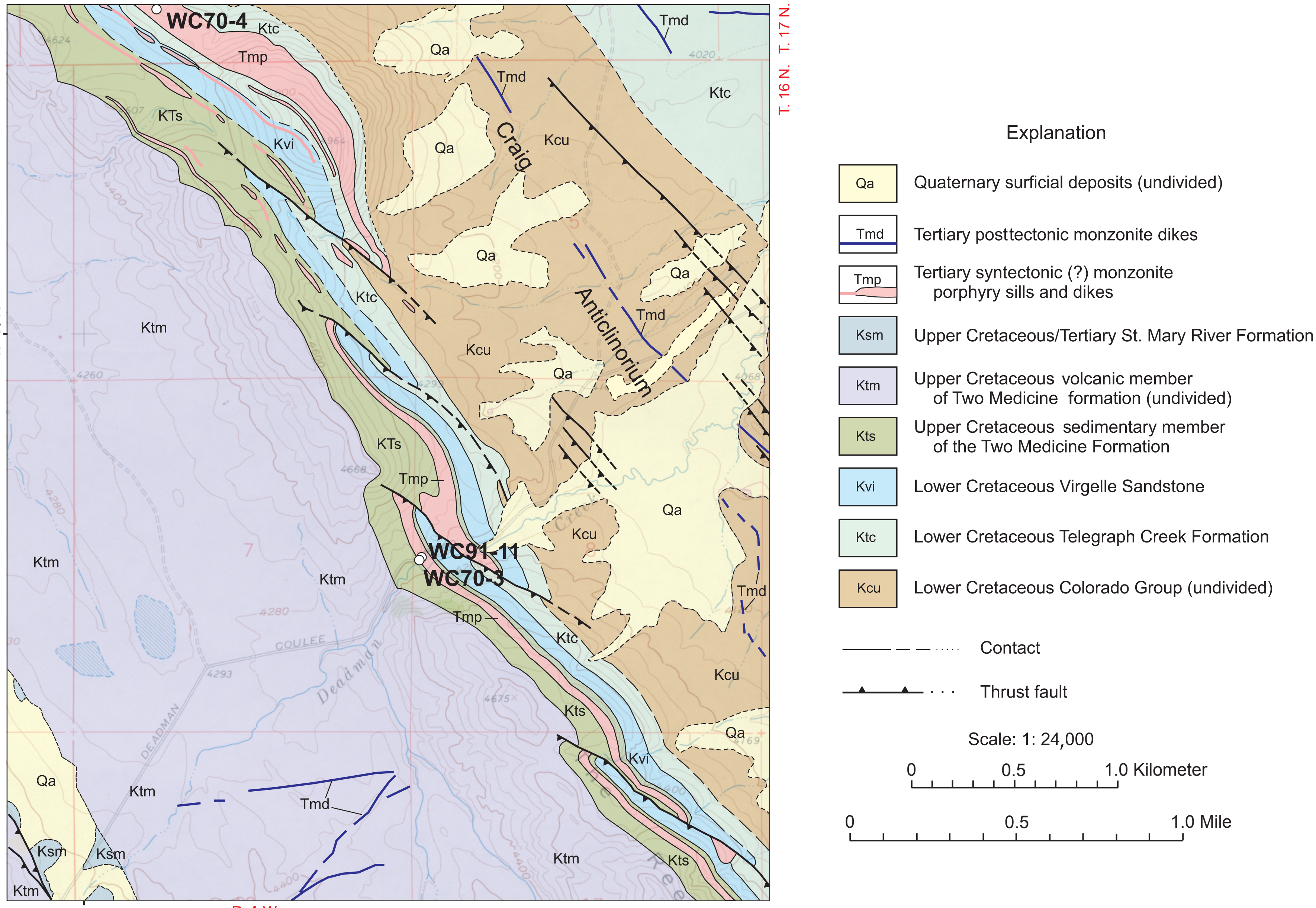

Figure 11. Simplified geologic map of part of the Comb Rock 7.5-minute quadrangle, Montana, showing the structural relations between monzonite porphyry sills and minor northwest-trending thrust faults along and near Deadman Coulee Road. Also shown are sample locations for samples WC70-3, WC70-4, and WC91-11. Modified from Schmidt (1972c)

the younger Adel Mountain volcanic rocks and the Finigan Mountain stock is a disconformable overlap and not the result of intrusion. Ambiguous field relations between the Finigan Mountain monzonite and the Adel Mountain Volcanics (see sample description in the Appendix), combined with the complex nature of the age spectrum, preclude its use in further constraining the age of the Adel Mountain Volcanics. Elsewhere in the field, sample WC70-2, from a hornblende-monzonite dike that clearly intrudes the Adel Mountain Volcanics, yielded a plateau age of 73.90±0.40 Ma (table 1; fig. 9*C*), whereas other monzonite intrusions are Tertiary, as discussed in the "Younger Intrusive Rocks" section.

Although the 75 to 72 Ma age of the volcanic rocks of the Adel Mountain field partly overlaps that of the volcanic member of the western facies of the Two Medicine Formation (80 to 74 Ma), published geochemical data (Lyons, 1944; Soward, 1975a; and Schmidt, 1978) suggest that the Adel Mountain volcanic rocks are typically alkaline and geochemically distinct from the largely subalkaline volcanic rocks of the Two Medicine Formation (fig. 10). Thus, field relations, geochemical data, and geochronologic data indicate that the Adel Mountain Volcanics are probably not lateral and temporal equivalents of the volcanic rocks of the Upper Cretaceous Two Medicine Formation, as has been suggested by some workers (King, 1997; Sears and others, 2000; and Sears, 2001).

Younger Intrusive Rocks

A number of younger, latest Cretaceous(?) and(or) Tertiary intrusive rocks of monzonite and quartz monzonite compositions are exposed in the vicinity of the Adel Mountain volcanic field. Some of these intrusions are northwest- and northeast-trending conjugate dikes that clearly crosscut the western part of the Adel Mountain volcanic field, as well as folds and thrust faults of the Montana disturbed belt (fig. 2). Hence, they clearly postdate Adel Mountain volcanism and thrust belt contractional deformation. They are thought to represent the youngest episode of igneous activity in the area (Schmidt, 1978). Other intrusions, also exposed generally west of the Adel Mountain volcanic field, are found as sills, sill-like bodies, and somewhat irregular to complex intrusions in folds. Some of the sill-like intrusions are mapped as having been cut by thrust faults (fig. 11). The spatial relationship between these intrusions with thrust faults and folds, the apparent fault offset shown by some intrusions, and the overall geometry of the intrusions suggests that at least some of these monzonite sills may be pretectonic or syntectonic with respect to fold and thrust deformation. In contrast, some dikelike intrusions are mapped as having been intruded along fault planes. Dikelike intrusions that intrude or cut the fault planes must postdate thrusting. Prior to the original K-Ar dating done for this study in the early 1970s, the geologic age of the monzonite intrusions was not known with any certainty, although the intrusions were considered to be Paleocene in age by Schmidt (1978). Thus, isotopic dates from these intrusions, if their exact relationship to folding and faulting can be unambiguously determined, have the potential to place important constraints on the age of thrust-belt deformation in this part of the disturbed belt. Their significance with respect to this problem, based in large part on preliminary and(or) unpublished K-Ar dating, has been discussed by a number of authors (Schmidt, 1978; Harlan, 1986; Whipple and others, 1987; Constenius, 1996).

In the following discussion, we will first discuss geologic map data which support the idea that some of the monzonite intrusions in this area appear to be pretectonic and(or) syntectonic with respect to contractional deformation. Next, we will present map and field evidence indicative of a post-thrusting origin for some intrusions. Finally, we will describe a complex situation in which a monzonite intrusion, whose geologic map pattern is largely that of an apparent pretectonic or syntectonic sill, is actually shown to postdate fold and thrust deformation. This discussion will highlight the need for additional detailed field, structural, and geochronologic studies of these latest Cretaceous(?) to early Tertiary intrusions if they are going to be used to interpret the age of fold and thrust-belt deformation.

Apparent Prefolding or Synfolding Intrusions

Samples (WC70-3, WC70-4, and WC91-11) from two quartz monzonite intrusions exposed in the Comb Rock quadrangle west of the Adel Mountain volcanic field were dated by the K-Ar and $^{40}Ar/^{39}Ar$ isotopic dating methods (figs. 2, 11). The sills are exposed in west-dipping volcanic and volcaniclastic strata of the volcanic member of the western facies of the Upper Cretaceous Two Medicine Formation. Map relations and cross-sectional views of Schmidt (1972c) suggest that these sills and other nearby intrusions exposed in sections 31 of T. 17 N., R. 4 W. and 36 of T. 17 N., R. 5 W. and sections 6, 8, and 17 of T. 16 N., R. 4 W. either have been folded or were intruded along bedding-plane weaknesses in folds. Evidence for this interpretation arises largely from the concordant, sheetlike nature of most of these intrusions in map view, as their mapped geometry generally, though not perfectly, mimics the contacts of host strata (fig. 11). Similarly, intrusions in sections 23 and 33 in T. 17 N., R. 5 W., along the westernmost part of the Comb Rock quadrangle, are sill-like in map view and appear to wrap completely around the southeastern nose of a northwest-plunging syncline. This map pattern suggests that the sills may have been folded, but such interpretations of map pattern must be viewed with caution as paleomagnetic studies have shown that some post-tectonic sills merely mimic fold geometries during intrusion (Harlan and others, 1988; Harlan and others, 1995).

Possibly the most intriguing and structurally significant map relationships in this area, however, are found in sections 6, 8, and 17 of T. 16 N., and R. 4 W., in the southeastern part of the Comb Rock quadrangle where samples WC70-3, and WC91-11 were collected (fig. 11). Geologic mapping by Schmidt (1972c) appears to show that these monzonite porphyry sills are cut in

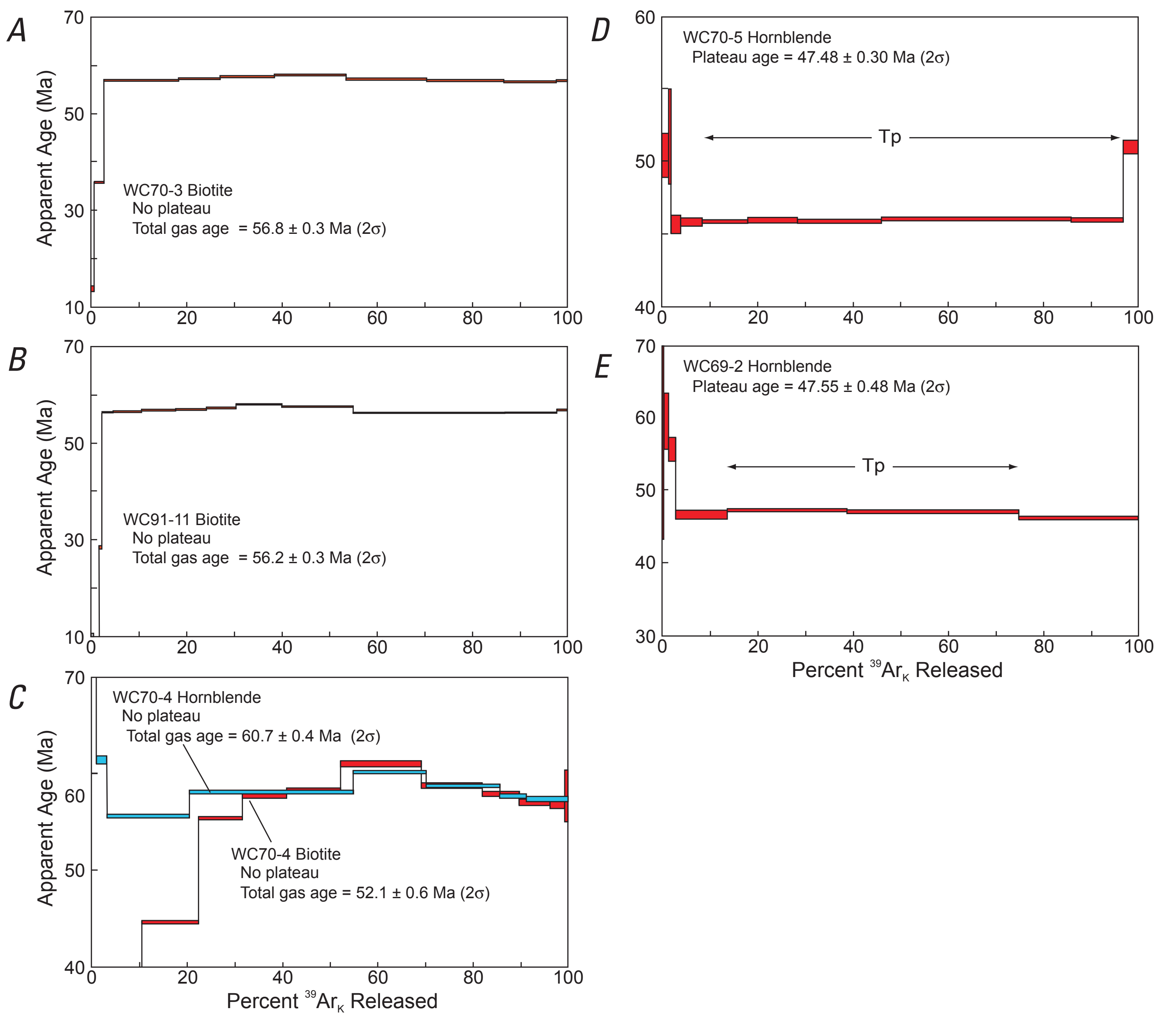

Figure 12. $^{40}Ar/^{39}Ar$ age spectra for hornblende and biotite concentrates from Tertiary sills and dikes. *C*, blue, hornblende; red, biotite.

several places by minor, right-displacement, left-stepping en-echelon thrust faults along the western margin of the Craig anticlinorium. If these sills are actually cut by the thrust faults, this relationship would suggest that sill emplacement predates or is synchronous with fold and thrust deformation.

A K-Ar biotite date from sample WC70-3 gives an apparent age of 55.8±1.4 Ma, whereas sample WC70-4 gives strongly discordant hornblende and biotite K-Ar dates of 64.8±1.6 Ma and 54.9±1.6 Ma, respectively (table 1). $^{40}Ar/^{39}Ar$ analyses of two different samples (WC70-3 and WC91-11; figs. 12*A* and 12*B*, respectively) from the same sill give somewhat discordant age spectra, with essentially identical total gas ages of about 56.8±0.3 Ma and 56.2±0.3 Ma. The total gas ages are in excellent agreement with the K-Ar date of 55.8 (table 1) from sample WC70-3. The overall hump-shaped spectra are probably the result of minor chloritization of the biotite. We cautiously interpret the $^{40}Ar/^{39}Ar$ total gas ages to represent the geologic age for these samples.

In contrast, $^{40}Ar/^{39}Ar$ dates from the hornblende and biotite from sample WC70-4 (fig. 12*C*) give strongly discordant and complex age spectra with significantly different total gas ages of 60.7±0.4 Ma and 52.1±0.6 Ma, respectively. The observed disparity in the total gas ages is similar in magnitude to that observed in the K-Ar dates from the same samples. The hornblende age spectrum gives anomalously old apparent ages in the initial low-temperature steps of the heating experiment, followed by a U-shaped trough with a minimum apparent age of about 55.8 Ma, followed by intermediate and high temperature steps with an overall hump-shaped age pattern. Although partly U-shaped, this age spectrum is not easily interpreted in terms of excess argon but could presumably reflect the incorporation of both excess ^{40}Ar and(or) ^{40}Ar loss. The biotite from WC70-4 also yields a strongly discordant and hump-shaped age spectrum clearly showing the effects of extensive chloritization. We speculate that the profound disturbance of both the hornblende and biotite $^{40}Ar/^{39}Ar$ systems could be the result of fluid flow accompanying fold and thrust deformation, although we have no specific field or petrographic evidence to demonstrate that this has occurred. Unfortunately, the complexities in both the hornblende and biotite samples from WC70-4 and the highly discordant nature of the total gas dates preclude meaningful interpretations of the age of these samples, and the dates should not be used in discussions of the age of fold and thrust-belt deformation in this part of the disturbed belt.

Determining the isotopic ages of sills in the Comb Creek quadrangle is somewhat problematic given the discordant nature shown by samples from all of the sills dated by the $^{40}Ar/^{39}Ar$ method. If we consider the approximate age of 56.8 and 56.2 Ma for samples WC70-3 and WC91-11 to be reasonable estimates for the age of these intrusions, and if these sills can be unambiguously determined to have predated fold and thrust-belt deformation, then geologic relations in this area may indicate that the waning stages of contractional deformation in this part of the Montana disturbed belt continued through the Paleocene and may have extended to as young as the Paleocene/Eocene boundary at about 55.5 Ma, relative to the Cenozoic time scale of Berggren and others (1995). However, we caution that these somewhat discordant ages may actually represent minimum values for the age of this deformational event, and we stress that better geochronologic data are needed to support this interpretation. Further, given the ambiguous and sometimes contradictory nature of map relations shown by the intrusions in this area, as described below, combined with the possibility that there may be multiple generations of latest Cretaceous(?) and early Tertiary monzonite intrusions in this part of the thrust belt with different relationships to fold and thrust-belt structures, the interpretation that fold and thrust deformation continued through to the Paleocene/Eocene boundary must be considered to be preliminary in nature. Confirmation of this interpretation will require additional high-precision isotopic dating of isotopically undisturbed samples whose relationship to fold and thrust-belt structures can be clearly demonstrated.

Apparent Postfolding Intrusions

Elsewhere in this area, the relationship between the quartz monzonite intrusions and the fold and thrust-belt structures is complex, ambiguous, and(or) contradictory. Some relationships appear to indicate that some monzonite intrusions postdate contractional deformation. For example, in sections 23 and 24 of T. 17 N., R. 5 W., a somewhat irregular intrusion appears to cut across fold structures and contacts of host sedimentary rocks, suggesting that it postdates deformation. Similarly, a monzonite intrusion exposed in sections 15 and 16 of T. 17 N., R. 5. W., in the northwestern part of the Comb Rock quadrangle, is mapped as having intruded along a thrust plane (Schmidt, 1972c). Hence, this monzonite dike likely postdates thrust faulting. Also, field relations elsewhere along the Eldorado thrust in Sheep Creek quadrangle south of Wolf Creek, Montana, indicate that a monzonite sill intrudes that fault and thus postdates thrust deformation (M.W. Reynolds, unpublished geologic mapping, 2000). Clearly, the map relations in this part of the disturbed belt indicate that the relationship between monzonite intrusion and folding and thrust deformation is complex and even contradictory. We suggest that these apparently contradictory map and field relations may provide evidence for multiple generations of early Tertiary monzonite intrusions that may be pretectonic, syntectonic, and posttectonic with respect to fold and thrust deformation.

Evidence for Postdeformation Monzonite Sill and Dike Intrusion along the Steinbach Thrust Fault

In the Johnson Mountain quadrangle, just west of the apparent pretectonic or syntectonic sills exposed in the Comb Rock quadrangle previously described, a monzonite intrusion provides critical field evidence that at least some of the intrusions that appear to predate or be synchronous with folding and faulting may actually postdate deformation. Original field notes of R.G. Schmidt describe this intrusion as a sill that was overridden by what is now called the Steinbach thrust fault (see sample description in the Appendix). In contrast, more recent geologic mapping by Mudge and others (1982) shows this intrusion to be a dike that cuts the Steinbach thrust fault. Regionally, the relationship between sill intrusion and faulting is significant because the Steinbach thrust fault is one of the easternmost and youngest thrust faults of the Montana disturbed belt.

Recent discovery of an unpublished geologic map fragment of R.G. Schmidt (unpublished mapping, 1969) demonstrates that the relation between monzonite intrusion and deformation at this locality is complex. This map is critical to deciphering the relationship between monzonite intrusion and faulting in this area. At this locality, a monzonite porphyry is a complex intrusion that is sill-like in part, with the main mass of the intrusion having the map appearance of having been cut by the Steinbach thrust fault (fig. 13). Along the northern edge of the main intrusive mass, however, the “sill” cuts abruptly across the trace of the fault as a high-angle dike. Along the southern side of Sunrise Hill, generally red, argillaceous, sedimentary strata of the Spokane Formation of the Middle Proterozoic Belt Supergroup in the hanging wall of the fault have been baked in a gray zone along the trace of the fault. Examination of unpublished field photographs of R.G. Schmidt indicates that the sill-like part of this intrusion, exposed in a small drainage just south of Montana Highway 200, has not been significantly deformed by thrusting (fig. 14). In contrast, the host sedimentary strata above and below the sill are strongly sheared (figs. 14 and 15). Together, the combination of the observation that the dike cuts the Steinbach thrust plane, the evidence of baked sedimentary strata in the hanging wall of the fault adjacent to the intrusion, and the apparent lack of deformation of the intrusion provide strong evidence that emplacement of the monzonite postdates faulting. Apparently, the intrusion exploited favorable sedimentary horizons during intrusion but largely swelled and “ponded” in the footwall of the thrust against the fault plane, thus baking the sedimentary rocks in the

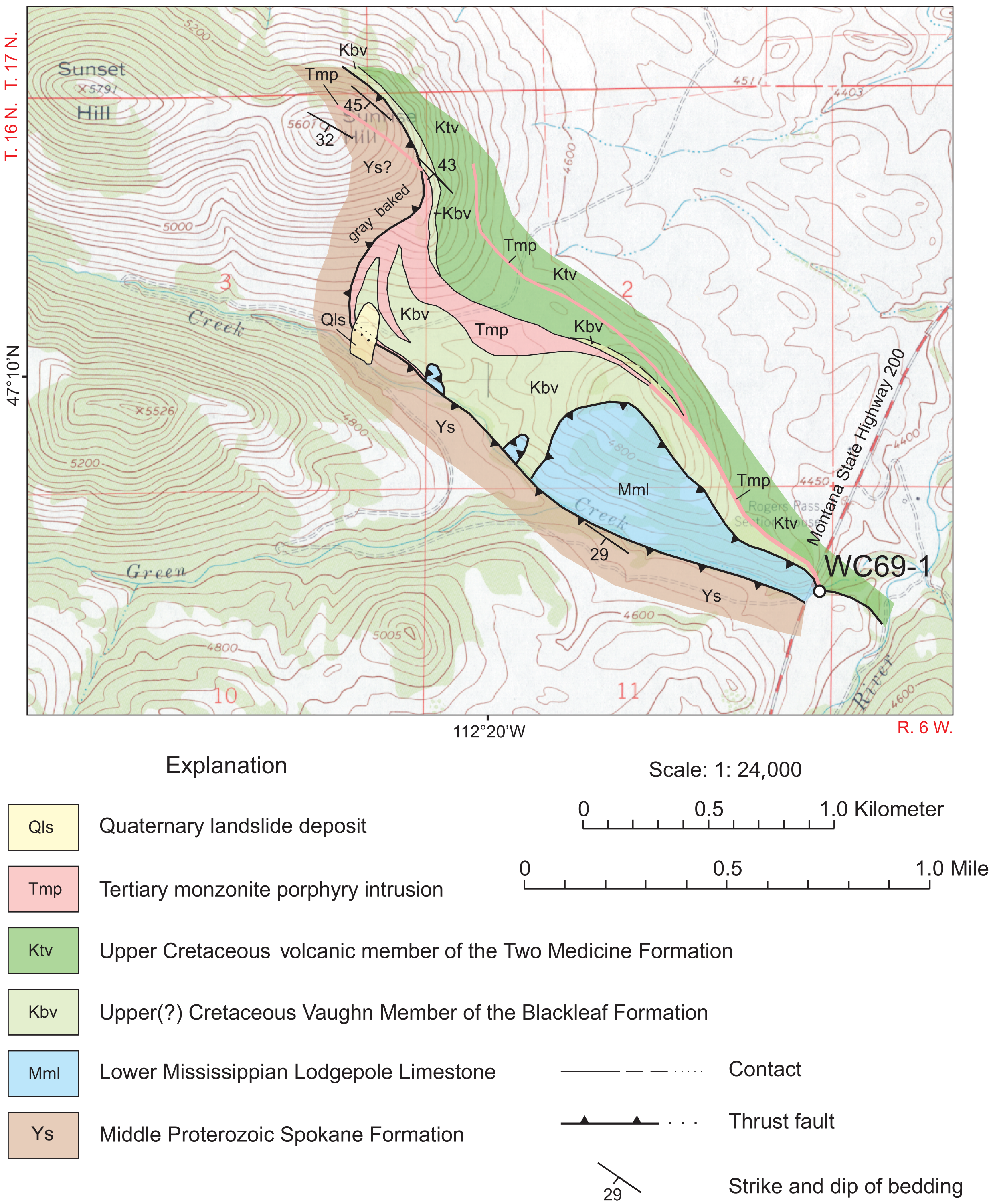

Figure 13. Geology of part of the Johnson Mountain 7.5-minute quadrangle, Montana, showing structural relations between monzonite intrusion and the Steinbach thrust fault. Also shown is the location of K-Ar sample WC69-1. Along the Montana State Highway 200, the intrusion is sill-like and appears to be cut by the Steinbach thrust fault. To the northwest, the sill bifurcates, swells, and appears to be "ponded" against the fault plane in the footwall of the thrust. Along the eastern side of Sunrise Hill, the intrusion cuts across the trace of the fault as a high-angle intrusion. In the hanging wall of the fault, the normally red argillaceous sediments of the Middle Proterozoic Spokane Formation have been altered to a gray color by the thermal effects of the intrusion. The observation that the intrusion cuts the fault, the presence of baked sediments in the hanging wall of the fault, and the undeformed nature of the intrusion, as shown by photographs in figures 14 and 15, indicate that the monzonite porphyry postdates thrust faulting at this locality. Unpublished geologic map of R.G. Schmidt (undated, probably 1969).

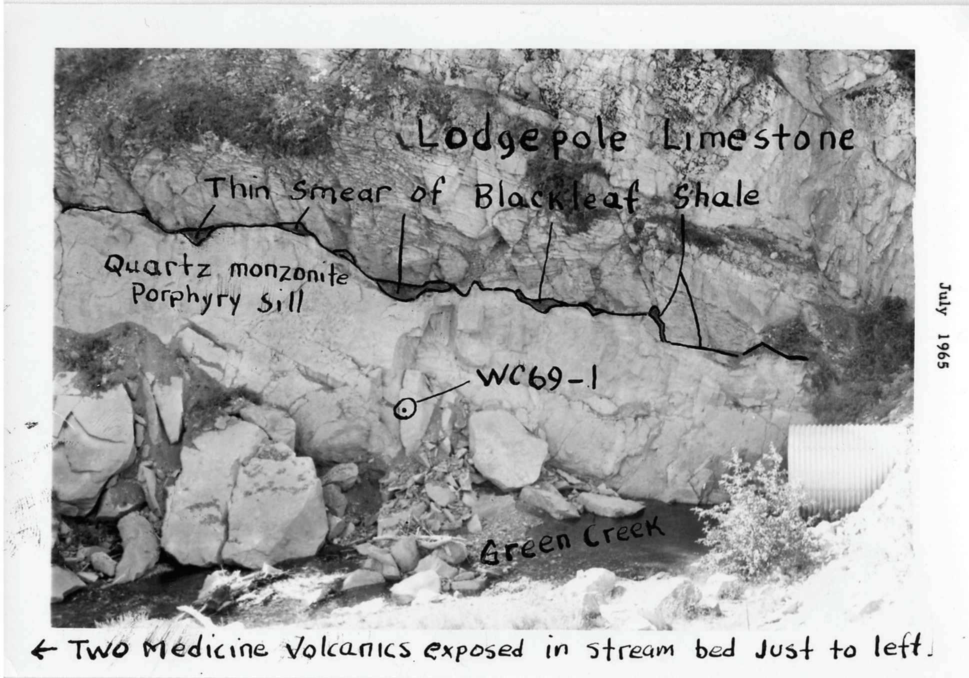

Figure 14. Photograph of quartz monzonite porphyry sill exposed in the bottom of Green Creek along Montana State Highway 200, approximately 1 mile southwest of the Middle Fork of the Dearborn River. Exposed above the sill are strongly deformed strata of the Lower Mississippian Lodgepole Limestone, along with thin smears of shale of the Lower and Upper(?) Cretaceous Black Leaf Formation of the Colorado Group. The base of the sill is not exposed, but volcanic conglomerate of the volcanic member of the Upper Cretaceous Two Medicine Formation is exposed in the streambed just to the left of the photograph. Also shown is the location of the part of the outcrop from which sample WC69-1 was collected. Unpublished photograph by R.G. Schmidt (dated 1965).

hanging wall of the fault. The complex relationship shown by this intrusion calls into question the viability of interpretations of the pretectonic or syntectonic interpretations of sills described above, as similar intrusive processes could have operated along those structures.

Sample WC69-1 from this sill gave a K-Ar date of 59.6±1.6 Ma (table 1). This age is similar to apparent ages from the other samples of the Tertiary quartz monzonites dated by both the K-Ar and $^{40}Ar/^{39}Ar$ methods, as described previously. Unfortunately, we were unable to obtain a split of sample WC69-1 for $^{40}Ar/^{39}Ar$ dating. Given some of the complications in $^{40}Ar/^{39}Ar$ age spectra seen in other samples, it is difficult to determine how reliable the 59.6 Ma date may actually be. However, R.G. Schmidt's field notes for this sample (unpublished field notes, 1969; see locality description in the Appendix) indicate that, in addition to biotite, the sill also contains sanidine phenocrysts up to 2.5 cm long. Because sanidine retains ^{40}Ar more effectively than biotite (Snee, 2002), additional $^{40}Ar/^{39}Ar$ dating of such material, if sufficiently fresh and unaltered, could provide critical information regarding the reliability of isotopic ages for the monzonite and quartz monzonite sills and the age of contractional structures in this part of the disturbed belt. If this age is accurate, however, the postfaulting relationship described here indicates that folding and thrusting may have ended by about 60 Ma.

The complex field relations shown by the monzonite intrusion described here highlight the problematic nature of trying to determine the timing of fold and thrust deformation based solely on interpretations of geologic maps. Careful examination of intrusive relations and fold/fault structures will be needed in order to fully understand the relationships between monzonites and contractional deformation. If the relationships between sill intrusion and folding/faulting can be unambiguously determined from a number of localities, they have the potential to place critical brackets on the timing of fold and thrust-belt deformation in this part of Montana.

Younger Posttectonic Monzonite Dikes

Two samples (WC70-5 and WC69-2) from the unambiguously posttectonic hornblende monzonite dikes were dated by the K-Ar and $^{40}Ar/^{39}Ar$ methods. Sample WC70-5 is from a prominent ridge-forming ("Rattlesnake Reef") southwest-trending dike that cuts Upper Cretaceous volcanic and volcaniclastic strata of the Two Medicine Formation as well as several disturbed belt folds (fig. 2). Elsewhere in close proximity to sample WC70-5, conjugate dikes of similar composition and northwest trend cut thrust faults, including the easternmost thrust faults along the western margin of the Adel Mountain volcanic field (fig. 2). Sample WC69-2 is from a northwest-trending dike that clearly cuts the trace of the Steinbach thrust fault (fig. 2). K-Ar dates from the two samples yield apparent ages of 50.4±1.2 Ma

(WC70-5) and 47.5±1.3 Ma (WC69-2) (table 1). $^{40}Ar/^{39}Ar$ dates for hornblende separates from these two samples yield slightly U-shaped age spectra, but both samples yield plateau segments with essentially identical apparent ages of 47.48±0.30 Ma (WC70-5; fig. 12*D*) and 47.55±0.48 Ma (WC69-2; fig. 12*E*). The posttectonic nature of these dikes and the $^{40}Ar/^{39}Ar$ dates indicate that fold and thrust deformation of the Montana disturbed belt had clearly ceased by the early middle Eocene emplacement of the monzonite dikes. Dike emplacement is probably correlative with the incipient stages of Tertiary crustal extension across this part of northwestern Montana (Constenius, 1996). Other volcanic fields that were emplaced during this time include rocks of the central Montana alkalic province, the Lowland Creek Volcanics, the Absaroka Volcanic Supergroup, and the Challis Volcanics (L.W. Snee, unpub. data, 2005).

Summary and Conclusions

$^{40}Ar/^{39}Ar$ and K-Ar isotopic dates from the Adel Mountain Volcanics clearly demonstrate that the volcanic rocks are Late Cretaceous in age and not Tertiary as proposed by some workers. Although the lower age limit for the Adel Mountain Volcanics is not well constrained, data presented here are consistent with the initiation of volcanism beginning at about 76 Ma. $^{40}Ar/^{39}Ar$ dates from dikes, sills, and laccoliths, including intrusions thought to represent the latest stage of igneous activity in the field, are fairly tightly clustered between 74.74 and 73.17 Ma. Overall, the geochronologic data are consistent with a temporally limited range of activity between about 76 and 73 Ma and might have spanned as little as 2 to 3 m.y. This is significantly less than the proposed 10-m.y. span proposed by Gunderson and Sheriff (1991) based on two K-Ar dates. Regional field relations, geochronologic data, and geochemical data indicate that the Adel Mountain Volcanics and the volcanic member of the western facies of the Two Medicine Formation are not laterally related.

Refined isotopic dating both confirms and slightly refines the age of the Adel Mountain paleomagnetic reference pole for cratonic North America. The original age assignment was 75 Ma based on the average of two widely disparate K-Ar dates reported by Sheriff and Gunderson (1990) and Gunderson and Sheriff (1991). The new dates suggest that the age of the Adel Mountain Volcanics pole is probably best estimated as approximately 74 Ma, given that the estimate of the pole position is based on a mixture of lava flows and dikes. The dates are also consistent with the observation that the Adel Mountain paleomagnetic data are exclusively of normal polarity and that the proposed span of activity (2 to 3 m.y.) is entirely within normal polarity Chron 33. Although a much more restrictive range of igneous activity is suggested by our new geochronologic data, the span of ages is consistent with the suggestion that the Adel Mountain paleomagnetic data of Gunderson and Sheriff (1991) adequately average paleosecular variation and thus represent the best estimate of the Late Cretaceous reference pole position for North America.

Structural relations within the Adel Mountain volcanic field are consistent with eruption of lava flows and dike and sill emplacement syntectonically with respect to Laramide contractional deformation. Along the southern margin of the field, the volcanics unconformably overlie and are intruded across fold axes and thrust faults, whereas along the western margin of the field, Upper Cretaceous strata of the Two Medicine Formation have been thrust eastward over the Adel Mountain Volcanics (Schmidt, 1972a, 1972b; Schmidt, 1978; M.W. Reynolds unpub. data, 1998 [for south part of the field]) and the volcanic rocks have been folded by blind thrusts. To the east, however, the volcanic rocks are essentially undeformed (Soward, 1975a, 1975b) consistent with their location east of the main zone of disturbed belt deformation. The isotopic dates reported here for the Adel Mountain Volcanics and syntectonic intrusions west of the field may indicate that contractional deformation in this area of the disturbed belt clearly extended to the latest Cretaceous. Assigning a younger age limit for fold and thrust deformation, however, is problematic. If some monzonites can be shown to predate or be

Figure 15. Panorama showing geologic relations between the monzonite porphyry sill and the Steinbach thrust fault along Montana State Highway 200 about 1 mile south of the bridge across the Middle Fork of the Dearborn River, Johnson Mountain quadrangle. From left to right, the photograph shows strongly deformed and sheared strata of the Lower Mississippian Lodgepole Limestone in the hanging wall of the thrust, strongly sheared black shale of the Lower and Upper(?) Cretaceous Blackleaf Formation of the Colorado Group, the monzonite porphyry sill, and a thin septum of Kootenai Formation rocks beneath the sill. A thin septum of Kootenai rocks is found within the sill. Unpublished photographs of R.G. Schmidt (dated 1965).

synchronous with folding and faulting, then contractional deformation may have extended to as young as the Paleocene/Eocene boundary at about 55.5 Ma. In contrast, a single K-Ar date from an intrusion that clearly postdates deformation indicates contractional deformation may have ceased by 60 Ma. Because of ambiguities regarding the relationships between sill intrusion and folding/faulting in this area, the possibility of multiple generations of pretectonic, syntectonic, or posttectonic early to latest Cretaceous early Tertiary sills, and complexities in the argon isotopic systematics shown by all samples dated in this study, this interpretation must be viewed with caution. A more precise age determination for this deformation may be possible by careful examination of field relations of the monzonite intrusion from which sample WC69-1 was collected, combined with $^{40}Ar/^{39}Ar$ dating of sanidine phenocrysts reportedly present in this sample. We stress that careful examination of the relationships between igneous intrusions and folding and thrusting at a number of localities will be needed in order to more fully and accurately constrain the age of fold and thrust deformation in this part of the Montana disturbed belt.

Field relations among younger monzonite northwest- and southwest-trending dikes that cut the Adel Mountain Volcanics, Cretaceous to lower Tertiary sedimentary strata, and disturbed belt folds and thrust faults clearly indicate that contractional deformation had ceased prior to early middle Eocene dike emplacement at about 47 Ma. This episode of dike emplacement is consistent with a widespread episode of magmatism that affected large areas of the northern Cordillera and includes rocks of the central Montana alkalic province, the Lowland Creek Volcanics, the Absaroka Volcanic Supergroup, and Challis Volcanics. This magmatic episode is temporally associated with gravitational collapse of the Cordilleran orogenic wedge and the onset of widespread crustal extension in the northern Rocky Mountains.

Selected References

Beall, J.J., 1972, Pseudo-rhythmic layering in the Square Butte alkali-gabbro laccolith: American Mineralogist, v. 57, p. 1294–1302.

Beall, J.J., 1973, Mechanics of intrusion and petrochemical evolution of the Adel Mountain Volcanics: Missoula, University of Montana, unpub. Ph.D. dissertation, 101 p.

Bellon, H., Houlgatte, E., Gouronnec, P., Blanchet, R., Tardy, M., Tour Du Pin, H., Vot, M., and Villien, A., 1989, Mesozoic and Cenozoic magmatism in the Overthrust Belt (North American Cordilleras, U.S.A.). ^{40}K-^{40}Ar ages and geodynamic significance: Bulletin of the Geological Society of France, v. 8, p. 627–637.

Berggren, W.A., Kent, D.V., Swisher, C.C., III, and Aubry, M.-P., 1995, A revised Cenozoic geochronology and chronostratigraphy, *in* Berggren, W.A., Kent, D.V., Aubry, M.-P., and Hardenbol, J., eds.,Geochronology time scales and global stratigraphic correlation: Society of Economic Paleontology and Mineralogy Special Publication 54, p. 129–212.

Chadwick, R.A., 1972, Volcanism in Montana: Northwest Geology, v. 1, p. 1–20.

Constenius, K.N., 1996, Late Paleogene extensional collapse of the Cordilleran foreland fold and thrust belt: Geological Society of America Bulletin, v. 108, p. 20–39.

Cunningham, B.L., 1999, Petrogenesis of the Adel Mountains volcanic field, central Montana: Missoula, unpub. Master's thesis, University of Montana, 82 p.

Cunningham, B.L., and Hyndman, D.W., 1999, Petrogenesis of the Adel Mountains, central Montana; evidence for magma mingling: Geological Society of America Abstracts with Programs, v. 31, no. 4, p. 9.

Dalrymple, G.B., and Lanphere, M.A., 1969, Potassium-argon dating: San Francisco, W.H. Freeman, 251 p.

Fleck, R.J., Sutter, J.F., and Elliott, D.H., 1977, Interpretation of discordant $^{40}Ar/^{39}Ar$ age spectra of Mesozoic tholeiites from Antarctica: Geochimica et Cosmochimica Acta, v. 41, p. 15–32.

Gunderson, J.A., 1989, Paleomagnetism of the Late Cretaceous-Paleocene Adel Mountain Volcanics, west-central Montana: Missoula, University of Montana, unpub. Master's thesis, 241 p.

Gunderson, J.A., and Sheriff, S.D., 1991, A new Late Cretaceous paleomagnetic pole from the Adel Mountains, West Central Montana: Journal of Geophysical Research, v. 96, p. 317–326.

Harlan, S.S., 1986, Timing of deformation along the leading edge of the Montana disturbed belt, northern Crazy Mountains Basin, Montana: Bozeman, Montana State University, Master's thesis, 87 p.

Harlan, S.S., Geissman, J.W., Lageson, D.R., and Snee, L.W., 1988, Paleomagnetic and isotopic dating of thrust belt deformation along the eastern edge of the Helena salient, northern Crazy Mountains, Montana: Geological Society of America Bulletin, v. 100, p. 492–499.

Harlan, S.S., Snee, L.W., Mehnert, H.H., Sheriff, S., and Schmidt, R.G., 1991, New $^{40}Ar/^{39}Ar$ isotopic ages from the Adel Mountain volcanics— Implications for the relationship between deformation and magmatism in the Montana disturbed belt, western Montana: Geological Society of America Abstracts with Programs, v. 23, p. A136.

Harlan, S.S., Geissman, J.W., Henry, C.D., and Onstott, T., 1995, Paleomagnetism and $^{40}Ar/^{39}Ar$ geochronology of gabbro sills at Mariscal Mountain anticline, southern Big Bend National Park, Texas—Implications for the timing of Laramide tectonism and vertical axis rotations in the southern Cordilleran Orogenic Belt: Tectonics, v. 14, p. 307–321.

Hyndman, D.W., and Alt, D., 1987, Radial dikes, laccoliths and gelatin models: Journal of Geology, v. 95, p. 763–774.

Ingamells, C.O., 1970, Lithium metaborate flux in silicate analysis: Analytica Chimica Acta, v. 52, p. 323–334.

Irvine, T.N., and Baragar, W.R.A., 1971, A guide to the chemical classification of the common volcanic rocks: Canadian Journal of Earth Sciences, v. 8, p. 523–548.

Irving, A.J., and O'Brien, H.E., 1994, Geochemistry of the mafic shoshonitic Adel Mountain Volcanics, Montana—Late Cretaceous arc-related magmatism with a lithospheric imprint: Geological Society of America Abstracts With Programs, v. 26, p. A–40.

King, J.T., 1997, Facies analysis of the volcaniclastic Two Medicine Formation, Wolf Creek, Montana: Missoula, University of Montana, unpub. Master's thesis, 54 p.

LaBranche, J.V., 1999, Sedimentary deposits and processes of the Late Cretaceous Adel Mountain volcaniclastic apron, west-central Montana: Bozeman, Montana State University, unpub. Master's thesis, 114 p.

Lo, C.H., and Onstott, T.C., 1989, 39Ar recoil artifacts in chloritized biotite: Geochimica et Cosmochimica Acta, v. 53, p. 2607–2711.

Lyons, J.B., 1944, Igneous rocks of the northern Big Belt Range, Montana: Geological Society of America Bulletin, v. 55, p. 445–472.

McIntyre, D.B., 1963, Precision and resolution in geochronometry, *in* Albritton, C.C., ed., The fabric of geology: Reading, Mass., Addison-Wesley, p. 112–134.

Mudge, M.A., Earhart, R.L., Whipple, J.W., and Harrison, J.E., 1982, Geologic structure map of the Choteau 1°×2° quadrangle: U.S. Geological Survey Miscellaneous Investigations Map, I–1300, scale: 1:250,000.

Renne, P.R., Swisher, C.C., Deino, A.L., Karner, D.B., Owens, T.L., and DePaolo, D.J., 1998, Intercalibration of standards, absolute ages and uncertainties in $^{40}Ar/^{39}Ar$ dating: Chemical Geology, v. 145, p. 117–152.

Rogers, R.R., Swisher, C.C., III, and Horner, J.R., 1993, $^{40}Ar/^{39}Ar$ age and correlation of the nonmarine Two Medicine Formation (Upper Cretaceous), northwestern Montana, U.S.A.: Canadian Journal of Earth Sciences, v. 30, p. 1066–1075.

Samson, S.D., and Alexander, E.C., Jr., 1987, Calibration of the interlaboratory ^{40}Ar-^{39}Ar dating standard, MMhb-1: Chemical Geology, v. 66, p. 27–34.

Schmidt, R.G., 1972a, Geologic map of the Wolf Creek quadrangle, Lewis and Clark County, Montana: U.S. Geological Survey Quadrangle Map GQ–974, scale: 1:24,000.

Schmidt, R.G., 1972b, Geologic map of the Coburn Mountain quadrangle, Lewis and Clark and Cascade counties, Montana: U.S. Geological Survey Quadrangle Map GQ–975, scale: 1:24,000.

Schmidt, R.G., 1972c, Geologic map of the Comb Rock quadrangle, Lewis and Clark Counties, Montana: U.S. Geological Survey Quadrangle Map GQ–976, scale: 1:24,000.

Schmidt, R.G., 1977, Geologic map of the Craig quadrangle, Lewis and Clark and Cascade counties, Montana: U.S. Geological Survey Quadrangle Map GQ–1411, scale: 1:24,000.

Schmidt, R.G., 1978, Rocks and mineral resources of the Wolf Creek area, Lewis and Clark and Cascade Counties, Montana: U.S. Geological Survey Bulletin 1441, 91 p.

Sears, J.W., 2001, Emplacement and denudation history of the Lewis-Eldorado thrust slab in the northern Montana Cordillera, USA—Implications for steady-state orogenic processes: American Journal of Science, v. 301, p. 359–373.

Sears, J.W., Hendrix, M., Waddell, A., Webb, B., Nixon, B., King, T., Roberts, E., and Lerman, R., 2000, Structural and stratigraphic evolution of the Rocky Mountain foreland basin in central-western Montana, *in* Roberts, S., and Winston, D., eds., Geologic field trips, western Montana and adjacent areas: Rocky Mountain Section of the Geological Society of America, University of Montana, p. 131–155.

Sheriff, S.D., and Gunderson, J.A., 1990, Age of the Adel Mountain volcanic field, west-central Montana: Isochron/West, no. 56, p. 21–23.

Snee, L.W., 2002, Argon thermochronology of mineral deposits—A review of analytical methods, formulations, and selected applications: U.S. Geological Survey Bulletin 2194, 39 p.

Soward, K.S.,1975a, Geologic map of the Rocky Reef quadrangle, Cascade County, Montana: U.S. Geological Survey Quadrangle Map GQ–1240, scale: 1:24,000.

Soward, K.S.,1975b, Geologic map of the Hardy quadrangle, Cascade and Lewis and Clark Counties, Montana: U.S. Geological Survey Quadrangle Map GQ–1241, scale: 1:24,000.

Steiger, R.H., and Jäger, E., 1977, Subcommission on geochronology— Convention on the use of decay constants in geo- and cosmochronology: Earth and Planetary Science Letters, v. 36, p. 359–362.

Swenson, R.F., 1988, Adel Mountain Volcanics—A trip through geofantasyland: Missoula, University of Montana, unpub. senior thesis, 45 p.

Whipple, J.W., Mudge, M.R., and Earhart, R.L., 1987, Geologic map of the Rogers Pass area, Lewis and Clark County, Montana: U.S. Geological Survey Miscellaneous Investigations Series Map I–1642, scale: 1:48,000.

Whiting, C.K., 1977, Small laccoliths and feeder dikes of the northern Adel Mountain Volcanics: Missoula, University of Montana, unpub. Master's thesis, 74 p.

Appendix

Appendix—Sample Locations, Rock Descriptions, and Minerals Analyzed

Sample descriptions are based on field or published notes from various individuals who collected samples dated in this study. The sample locations and descriptions for samples 88AV-12 and 88AV01 were previously published by Sheriff and Gunderson (1990) and Gunderson and Sheriff (1991). Latitudes and longitudes for sample locations from R.G. Schmidt's samples (collected in 1969 and 1970), where reported, and Gunderson and Sheriff's (1991) samples are given to two places to the right of the decimal (that is, are reported to the nearest minute). Sample locations based on digitized map coordinates from field sheets are reported to four places to the right of the decimal (that is, are reported to the nearest second). Sample locations and rock descriptions are arranged in the order in which their analytical results are discussed in the text.

WC91-14b. Plagioclase. Devitrified, greenish-gray plagioclase-biotite tuff exposed in Burlington Northern ballast quarry along U.S. 287, approximately 1 mi south of Wolf Creek, Montana. Tuff contains abundant pumice and small lithic fragments. Euhedral, fresh-appearing biotite. Location: SE¼SW¼ sec. 2, T. 14 N., R. 4 W., Sheep Creek 7.5-minute USGS quadrangle, Lewis and Clark County, Montana. Latitude and longitude: 46.9943°N., 112.0731°W.

WC69-3. Biotite. Biotite-bearing augite trachybasalt. Lower part of Adel Mountain Volcanics of Lyons (1944). The rock is porphyritic with large phenocrysts of augite in a groundmass of labradorite, sanidine, augite, biotite, hornblende(?), quartz, magnetite, and apatite. Augite occurs in platelike crystals as much as 7 mm long. Biotite occurs in platelike crystals as much as 2 mm but generally less than 0.5 mm across. Sanidine and quartz mold between the other mineral constituents. Hornblende(?) is in small needlelike crystals less than 0.2 mm long. Sample is from a large angular block of trachybasalt in a thick layer of coarse volcanic breccia in the lower part of the Adel Mountain Volcanics. Location: East wall of the valley of the Missouri River, 3 to 6 m east of Frontage Road (formerly U.S. Highway 91), SW¼NE¼ sec. 20, T. 16 N., R. 2 W., Mid Canon 7.5-minute USGS quadrangle, Cascade County, Montana. Latitude and longitude not reported.

88AV-12. (Geochron Laboratories number R-8585). Whole rock. Fresh aphyric "shonkinite" flow. Location: lat 47.14°N., long 111.86°W., NW¼NE¼ sec. 21, T. 16 N., R. 2 W. Mid Canon 7.5-minute USGS quadrangle, Cascade County, Montana.

A-29a-89. Hornblende. Sample is from an igneous-textured apatite-magnetite hornblendite xenolith within a trachyandesite dike. Location: Exposed 0.5 km north of Hardy Bridge in NW¼ NW¼ sec. 2, T. 16 N., R. 2 W. Hardy 7.5-minute USGS quadrangle, Cascade County, Montana. Latitude and longitude: 47.1722°N., 111.6833°W.

A-31-89. Hornblende. Sanidine-phyric microsyenite dike. Dike contains large, flow-aligned, altered sanidine phenocrysts in a groundmass of hornblende, augite, feldspar, and oxides. Location: Exposed along Chestnut Valley road, 1 km northeast of Halfbreed Rapids in NE¼NE¼ sec. 36, T. 17 N., R. 2 W. Hardy 7.5-minute USGS quadrangle, Cascade County, Montana. Latitude and longitude: 47.1889°N., 111.7958°W.

WC70-2. Hornblende and Biotite. Hornblende-biotite monzonite dike. Dike intrudes Two Medicine Formation beneath Adel Mountain Volcanics of Lyons (1944). This dike extends southward into the Adel Mountain Volcanics. Dike is considered to be youngest or one of the youngest rock types in the Adel Mountain volcanic field (communication of Soward to Schmidt [1970]). Location: dike exposed along south side of Sheep Creek road in NE¼NE¼ sec. 36, T. 17 N., R. 2 W., Hardy 7.5-minute USGS quadrangle, Cascade County, Montana. Latitude and longitude: 47.1883°N., 111.7958°W.

AMV90-3. Biotite. Biotite-bearing trachybasalt dike. Location: northwest edge of Middle Creek Lake in NW¼ NW¼ sec. 25, T. 14 N., R. 1 W. Middle Creek Lake 7.5-minute USGS quadrangle, Lewis and Clark County, Montana. Latitude and longitude: 46.9361°N., 111.6833°W.

WC70-8. Biotite. Biotite-bearing trachybasalt dike in Adel Mountain Volcanics. Location: about 49 m above and south of Little Stickney Creek on nose of ridge in southeast corner of sec. 2, T. 15 N., R. 2 W., The Sawteeth 7.5-minute USGS quadrangle, Lewis and Clark County, Montana: Latitude and longitude: 47.0783°N., 111.8117°W.

WC70-6. Biotite. Biotite monzonite. Intrusive mass in Adel Mountain Volcanics. Probably part of Three Sisters stock near crest of ridge between Little Stickney Creek and North Fork of Stickney Creek. Location: SE¼NE¼SE¼ sec. 1, T. 15 N., R. 2 W., The Sawteeth 7.5-minute USGS quadrangle, Lewis and Clark County, Montana. Latitude and longitude: 47.0828°N., 111.7908°W.

88AV01. (Geochron Laboratories number B-8578). Biotite. "Shonkinite" dike with phenocrysts of plagioclase, clinopyroxene, very fresh biotite and magnetite. Location: This outcrop is obvious where the dike crosses the St. Peter Mission road in the NW¼NW¼ sec. 25, T. 18 N., R. 3 W., Cascade County, Montana. Latitude and longitude: 47.29°N., 111.94°W.

WC91-23. Biotite. Biotite (potassic) monzonite sill exposed in quarry, north side of Shaw Butte. Contains prominent euhedral clinopyroxene that is visually similar to that found in rocks exposed in Square Butte intrusion. The main mass of shonkinite does not contain obvious potassium-bearing phases; but diversely oriented leucocratic veins (1 to 8 cm wide), possibly representing late-stage melt segregation, contain euhedral platy minerals that appear to be biotite. Material collected is from freshly blasted leucocratic vein material exposed in the quarry. Location: Cascade Colony 7.5-minute USGS quadrangle, Cascade County, Montana. Latitude and longitude: 47.4742°N., 111.8345°W.

WC69-5. Hornblende. Hornblende monzonite stock underlying Finigan Mountain. Rock is porphyritic and includes phenocrysts of hornblende and andesine in a groundmass of

Table A1. K-Ar analytical data for samples from the Adel Mountain Volcanics and spatially related volcanic and intrusive rocks, north-central Montana.

[%, percent; moles/g, moles per gram; B, biotite; H, hornblende. Constants used in calculation of K-Ar date: $K^{40}\lambda_\varepsilon = 0.581\times10^{-10}$/yr; $\lambda_\beta = 4.962\times10^{-10}$/yr; $K^{40}K = 1.167\times10^{-4}$g/g]

Lab no.	Sample no.	Rock type	Material dated	K (%)	*Ar^{40} ($\times10^{-10}$ moles/g)	*Ar^{40} (%)	Age ± 2σ (Ma)
2056	WC69–3	Augite-biotite trachybasalt breccia	B	5.776	7.49	94.4	73.2±2.1
2228	WC70–2	Hornblende-biotite monzonite dike	H	1.581	2.10	93.2	75.0±2.3
2227	WC70–2		B	4.602	5.94	87.6	72.9±2.1
2272	WC70–8	Biotite-bearing trachybasalt dike	B	6.997	9.13	92.2	73.7±2.1
2407	WC70–5	Hornblende monzonite	H	0.606	0.54	85.6	50.4±1.2
2056	WC69–5	Hornblende monzonite	H	1.257	1.86	89.6	83.3±2.5
2357	WC70–6	Biotite monzonite	B	7.047	9.24	93.4	74.0±2.1
2059	WC69–1	Biotite-bearing quartz monzonite	B	5.164	5.43	86.5	59.6±1.6
2225	WC70–3	Biotite-bearing monzonite porphyry	B	6.856	6.74	90.0	55.8±1.4
2229	WC70–4	Biotite-hornblende quartz monzonite	H	0.854	0.98	77.0	64.8±1.6
2226	WC70–4	porphyry	B	3.196	3.09	65.5	54.9±1.6
2407	WC70–5	Hornblende monzonite	H	0.606	0.54	85.6	50.4±1.2
2055	WC69–2	Hornblende monzonite	H	0.698	0.58	88.3	47.5±1.3

andesine, sanidine, hornblende, biotite, quartz, magnetite, and apatite. Hornblende phenocrysts are in slender crystals as much as 5 mm, but generally 2 mm, long. The stock intrudes rocks of the Two Medicine Formation of Late Cretaceous age and may also intrude breccias and flows at or near the base of the Adel Mountain Volcanics. Poor exposures make it impossible to determine the true relation of the stock to the volcanics. Elsewhere in the region, stocks and plugs of hornblende monzonite intrude, and are therefore younger than, the Adel Mountain Volcanics. Although considered a stock by Schmidt (unpublished field notes), geologic mapping by Soward (1975b) describes this feature as a latite that includes vent breccia and probably extrusive breccia. Thus, this feature may be extrusive in origin. Location: South flank of Finigan Mountain in SE¼NE¼ sec. 13, T. 17 N., R. 2 W., Hardy 7.5-minute USGS quadrangle, Cascade County, Montana. Latitude and longitude not reported.

WC69-1. Biotite. Biotite-bearing monzonite porphyry sill exposed in a fault-bounded slice along the Steinbach thrust fault. Sample is from a 3- to 6-m-thick sill exposed in the south wall of valley of Green Creek, approximately 15 m east of Montana State Highway 200. Rock is porphyritic and includes phenocrysts of sanidine as much as 2.5 cm long enclosed in a groundmass of sanidine, oligoclase, quartz, biotite, hornblende, magnetite, and apatite. Hornblende crystals are altered to chlorite, calcite, and magnetite. In a road cut on the west side of the highway, the sill is underlain by a thin septum of red and purple shale of the Kootenai Formation of Early Cretaceous age. A thin septum of Kootenai Formation rocks is found within the sill. Regionally, the Blackleaf Formation rests on the Kootenai, and the sill appears to be intruded along the contact between these formations. Above the sill, Blackleaf beds are overridden by a 3- to 12-m wedge of Lodgepole Limestone of Early Mississippian age, and the wedge of Lodgepole Limestone is in turn overridden by rocks of the Middle Proterozoic Belt Supergroup that constitutes the main mass of the Steinbach thrust plate. On the east side of Highway 200, where the sample was obtained, a thin, discontinuous band of Blackleaf shale, less than 5 cm thick, is smeared between the top of the sill and the overriding wedge of Lodgepole Limestone; in places, limestone rests directly on the sill. At this locality, the base of the sill is not exposed, but Two Medicine Formation volcanics crop out in the stream bottom a short distance below the sill. It is R.G. Schmidt's interpretation in his original field notes that the sill is older than the thrusting and that the wedge formed by the Blackleaf Formation, the sill, the Kootenai Formation, and the wedge formed by the Lodgepole Limestone, are allocthonous slices caught along the Eldorado thrust and carried over the volcanic member of the Upper Cretaceous Two Medicine Formation. Elsewhere in the area, sills of quartz monzonite porphyry, similar in composition and texture to the sill described here, intrude rocks as young as the Willow Creek Formation of Late Cretaceous and Paleocene age, are folded and faulted, and are clearly older than the contractional deformation.

Although R.G. Schmidt's original notes consider the sill to have been deformed by thrust faulting, subquent unpublished mapping by R.G. Schmidt (1969) and Mudge and others (1982) show that the intrusion cuts the Steinbach thrust plate as a dike elsewhere in the Johnson Mountain quadrangle (fig. 13). Examination of original field photographs of R.G. Schmidt suggests that the sill is largely undeformed, although the host strata above and below the sill are strongly sheared (figs. 14, 15). The observation that the intrusion cuts the Steinbach thrust fault as a dike, has baked sedimentary strata of the Spokane Formation in the hanging wall of the fault, and is largely undeformed

Table A2. $^{40}Ar/^{39}Ar$ incremental heating data for samples of Adel Mountain Volcanics and spatially associated volcanic and intrusive rocks, north-central Montana.

[Note: $^{40}Ar_a$ is measured atmospheric argon used for mass-discrimination at time of analysis; $^{40}Ar_R$ is radiogenic ^{40}Ar in volts signal; ^{39}Ar is potassium-derived ^{39}Ar in volts signal; $^{40}Ar_R/^{39}Ar_K$ is the ratio of $^{40}Ar_R$ to $^{39}Ar_K$ after correction for mass-discrimination and interfering isotopes; $^{39}Ar/^{37}Ar$ = ratio of $^{39}Ar_K$ to $^{37}Ar_{Ca}$ (this value can be converted to the approximate K/Ca by multiplying by 0.52); %$^{40}Ar_K$ and %^{39}Ar are the percentage of radiogenic ^{40}Ar and percentage of total ^{39}Ar released in each temperature step. Temperature steps in boldface are those used in the calculation of the plateau age. Conversion of volts signal to moles Ar can be made using a conversion factor of 1.252×10^{-13} moles argon per volt of signal. Steps denoted by bold font are those used in calculation of the plateau dates as described in the text. Analytical details are available in Snee (2002)]

Temp (°C)	$^{40}Ar_R$	$^{39}Ar_K$	$^{40}Ar_R/^{39}Ar_K$	$^{39}Ar/^{37}Ar$	$^{40}Ar_R$ (%)	^{39}Ar (%)	Apparent age (Ma±1σ)
WC91–14b: plagioclase, ash-flow tuff, Two Medicine Fm; 202.8 mg; $^{40}Ar/^{36}Ar_a$ = 300.0; *J* value =0.006452±0.25% (1σ)							
900	1.1141	0.24333	7.224	0.17	82.9	30.0	82.18±0.14
1,000	0.58052	0.08806	6.592	0.17	91.0	10.7	75.14±0.57
1,050	0.47224	0.06792	6.953	0.17	90.2	8.3	79.17±0.75
1,100	0.89272	0.11863	7.526	0.16	91.3	14.5	85.54±0.23
1,150	1.0739	0.14280	7.521	0.16	92.7	17.4	85.48±0.21
1,200	0.52951	0.07290	7.263	0.16	92.7	8.9	82.62±0.60
1,300	0.60965	0.08348	7.303	0.16	91.7	10.2	83.06±0.46
Total gas			7.240				82.36±0.33
WC69–3: biotite; Adel Mountain Volcanics, flow, 61.8 mg; measured $^{40}Ar/^{36}Ar_a$ = 298.9; *J* value = 0.006287±0.25% (1σ)							
600	2.13686	0.35274	6.058	10.55	84.0	6.1	67.43±0.25
700	0.66739	0.09813	6.801	14.05	70.6	1.7	75.53±0.68
800	2.9969	0.42876	6.990	26.63	92.5	7.5	77.59±0.21
850	2.8905	0.41047	7.042	34.57	97.1	7.1	78.15±0.77
900	3.0016	0.43116	6.962	35.57	98.0	7.5	77.28±0.23
950	2.4035	0.35037	6.860	38.18	97.6	6.1	76.17±0.22
1,000	3.8807	0.55605	6.979	30.35	97.5	9.7	77.47±0.21
1,050	6.9201	1.0066	6.875	40.82	97.9	17.5	76.34±0.21
1,100	8.2579	1.2191	6.774	37.25	98.1	21.2	75.24±0.21
1,250	5.9763	0.88969	6.716	17.82	97.0	15.5	74.61±0.20
Total gas			6.814				75.67±0.24
88AV12: high-K whole rock; Adel Mountain Volcanics, flow, 261.4 mg; $^{40}Ar/^{36}Ar_a$ = 298.9; *J* value = 0.006375±0.25% (1σ)							
500	0.37203	0.07399	5.028	2.30	42.2	1.7	56.92±0.54
600	1.2470	0.19740	6.317	1.74	83.0	4.6	71.22±0.25
650	2.0636	0.31466	6.558	1.83	92.7	7.4	73.89±0.24
700	3.7946	0.57035	6.653	2.07	85.7	13.4	74.93±0.20
750	4.8581	0.72913	6.663	1.96	98.3	17.1	75.04±0.20
800	4.6473	0.68339	6.800	1.73	98.4	16.1	76.56±0.21
850	2.7495	0.39697	6.926	1.42	97.8	9.3	77.94±0.22
900	2.0170	0.29572	6.821	1.25	96.4	7.0	76.79±0.22
1,000	2.6936	0.41175	6.542	0.77	96.2	9.7	73.71±0.22
1,100	2.8889	0.44840	6.443	0.30	96.3	10.5	72.62±0.22
1,250	0.82701	0.12080	6.846	0.01	82.9	2.8	77.06±0.27
1,400	0.09120	0.01227	7.431	0.01	56.2	0.3	83.50±5.66
Total gas			6.639				74.78±0.23
A–29a–89: hornblende, Adel Mountain Volcanics dike, 220.2 mg; $^{40}Ar/^{36}Ar_a$ = 298.9; *J* value = 0.00756±0.25% (1σ)							
800	0.27715	0.02429	11.41	0.42	24.3	0.4	149.26±4.19
1,000	0.08423	0.01166	7.225	0.36	40.5	0.2	95.94±1.01
1,050	0.48299	0.08487	5.961	0.34	80.9	1.5	79.52±0.49
1,100	2.4891	0.44637	5.576	0.34	93.9	7.9	74.49±0.26
1,125	2.5173	0.44971	5.598	0.34	93.7	8.0	74.78±0.20
1,150	7.0510	1.2584	5.603	0.34	96.1	22.3	74.84±0.21
1,200	16.798	3.0054	5.589	0.34	94.1	53.3	74.66±0.20

Table A2. $^{40}Ar/^{39}Ar$ incremental heating data for samples of Adel Mountain Volcanics and spatially associated volcanic and intrusive rocks, north-central Montana—*Continued.*

Temp (°C)	$^{40}Ar_R$	$^{39}Ar_K$	$^{40}Ar_R/^{39}Ar_K$	$^{39}Ar/^{37}Ar$	$^{40}Ar_R$ (%)	^{39}Ar (%)	Apparent age (Ma±1σ)
A–29a–89 :hornblende, Adel Mountain Volcanics dike, 220.2 mg; $^{40}Ar/^{36}Ar_a$ = 298.9; *J* value = 0.00756±0.25% (1σ)—*Continued*							
1,250	1.6940	0.30350	5.581	0.32	87.9	5.4	74.55±0.20
1,350	0.21865	0.03867	5.654	0.14	88.0	0.7	75.51±1.02
1,450	0.08353	0.01546	5.402	0.17	72.5	0.3	72.21±3.21
Total gas			5.622				75.14±0.22
A–31–89: hornblende, Adel Mountain Volcanics dike, 298.9 mg; $^{40}Ar/^{36}Ar_a$ = 298.9; *J* value = 0.007399±0.3% (1σ)							
750	0.16402	0.03961	4.141	1.05	22.2	0.4	54.44±0.65
850	0.05351	0.01051	5.091	0.70	19.7	0.1	66.71±5.63
950	0.20590	0.03848	5.350	0.55	65.1	0.4	70.03±1.92
1,000	0.20558	0.03885	5.292	0.47	35.5	0.4	69.29±1.33
1,050	5.1114	0.91252	5.601	0.40	97.0	9.2	73.25±0.23
1,100	6.8045	1.2174	5.589	0.40	98.0	12.3	73.10±0.23
1,125	8.5788	1.5351	5.588	0.40	98.1	15.5	73.09±0.23
1,150	22.672	4.0530	5.594	0.40	94.9	40.9	73.16±0.23
1,200	8.4923	1.5148	5.606	0.38	96.4	15.3	73.32±0.23
1,250	2.8845	0.51205	5.633	0.27	94.0	5.2	73.66±0.23
1,350	0.08041	0.01583	5.079	0.09	51.1	0.2	66.55±1.04
1,450	0.05329	0.00930	5.728	.018	66.6	0.1	74.88±2.95
Total gas			5.588				73.09±0.24
WC70–2: hornblende, Adel Mountain Volcanics dike, 268.0 mg; $^{40}Ar/^{36}Ar_a$ = 298.9; *J* value = 0.006280±0.10% (1σ)							
600	0.02937	0.00477	6.161	0.76	11.7	0.1	68.48±9.73
700	0.12077	0.02696	4.479	1.21	21.8	0.5	50.04±0.19
750	0.05215	0.00839	6.213	0.55	31.1	0.1	69.05±1.72
800	0.05827	0.00926	6.292	0.48	37.3	0.2	69.91±1.06
850	0.08090	0.01123	7.206	0.47	21.1	0.2	79.84±1.63
900	0.11191	0.01545	7.242	0.40	17.7	0.3	80.23±0.12
950	2.9201	0.43356	6.704	0.40	81.5	7.3	74.40±0.11
1,000	5.8703	0.88382	6.642	0.40	92.4	14.9	73.72±0.11
1,025	8.0084	1.2026	6.659	0.40	88.0	20.3	79.91±0.11
1,050	10.995	1.6532	6.651	0.39	82.9	27.9	73.82±0.11
1,075	3.8646	0.57807	6.685	0.39	75.1	9.8	74.19±0.11
1,100	3.7723	0.56668	6.657	0.36	90.0	9.6	73.88±0.11
1,150	2.9923	0.45224	6.617	0.30	93.9	7.6	73.45±0.11
1,200	0.17279	0.03005	5.751	0.31	62.1	0.5	64.00±2.52
1,400	0.26345	0.05026	5.242	0.39	75.6	0.8	58.43±0.57
Total gas			6.631				73.60±0.14
WC70–2: biotite, Adel Mountain Volcanics dike, 57.2 mg; $^{40}Ar/^{36}Ar_a$ = 298.9; *J* value = 0.006358±0.25% (1σ)							
600	0.30355	0.46906	0.647	9.03	15.3	11.5	7.41±0.17
700	0.97334	0.16247	5.991	16.3	51.6	4.0	67.44±0.19
800	3.3740	0.49085	6.874	41.1	87.4	12.0	77.17±0.21
850	3.3242	0.45330	7.333	52.0	94.2	11.1	82.21±0.22
900	2.9311	0.40081	7.313	37.2	93.6	9.8	81.99±0.22
950	3.7660	0.46480	8.102	17.0	92.7	11.4	90.61±0.24
1,000	4.7151	0.60211	7.831	20.3	96.3	14.7	87.66±0.25
1,025	4.6714	0.64179	7.279	31.5	97.8	15.7	81.61±0.26
1,050	2.0902	0.29616	7.058	17.6	98.0	7.2	79.19±0.34
1,100	0.64271	0.09342	6.880	2.30	96.1	2.3	77.24±0.37

Table A2. $^{40}Ar/^{39}Ar$ incremental heating data for samples of Adel Mountain Volcanics and spatially associated volcanic and intrusive rocks, north-central Montana—*Continued.*

Temp (°C)	$^{40}Ar_R$	$^{39}Ar_K$	$^{40}Ar_R/^{39}Ar_K$	$^{39}Ar/^{37}Ar$	$^{40}Ar_R$ (%)	^{39}Ar (%)	Apparent age (Ma±1σ)
WC70–2: biotite, Adel Mountain Volcanics dike, 57.2 mg; $^{40}Ar/^{36}Ar_a$ = 298.9; *J* value = 0.006358±0.25% (1σ)—*Continued*							
1,150	0.09077	0.01190	7.631	0.30	89.1	0.3	85.47±3.12
Total gas			6.578				73.91±0.36
AMV90–3: biotite, Adel Mountain Volcanics dike, 268.0 mg; $^{40}Ar/^{36}Ar_a$ = 298.9; *J* value = 0.007671±0.25% (1σ)							
700	0.01263	0.00777	1.626	2.58	3.1	0.1	22.4±23.6
800	0.29849	0.10747	2.777	0.70	28.8	1.5	38.03±0.69
900	2.3264	0.42980	5.413	7.90	70.6	6.1	73.39±0.22
950	3.3881	0.60517	5.599	61.2	91.5	8.6	75.86±0.20
1,000	4.5471	0.81414	5.585	85.7	96.1	11.6	75.68±0.20
1,050	4.6451	0.83191	5.584	81.2	96.6	11.9	75.66±0.20
1,100	4.8164	0.86605	5.561	80.9	97.4	12.4	75.36±0.20
1,150	5.3426	0.96327	5.546	72.4	97.9	13.8	75.16±0.35
1,200	9.4088	1.7249	5.455	93.5	98.6	24.6	73.95±0.20
1,350	3.5276	0.64875	5.438	40.0	98.5	9.3	73.73±0.20
Total gas			5.474				74.20±0.29
WC70–8: biotite, Adel Mountain Volcanics dike, 62.4 mg; $^{40}Ar/^{36}Ar_a$ = 298.9; *J* value = 0.006309±0.25% (1σ)							
600	0.05020	0.02203	2.279	6.93	22.5	0.4	25.75±6.83
700	0.34589	0.05359	6.455	19.22	54.2	0.9	72.01±2.45
800	3.1326	0.47241	6.631	232	91.8	8.1	73.93±0.43
850	3.7037	0.56175	6.593	467	96.3	9.7	73.52±0.24
900	3.2120	0.48944	6.563	414	97.5	8.4	73.19±0.37
950	3.4972	0.52744	6.630	207	68.0	9.1	73.92±0.30
1,000	4.0418	0.61110	6.614	189	97.2	10.5	73.95±0.23
1,050	5.0878	0.76823	6.623	232	97.5	13.2	73.85±0.37
1,100	12.462	1.8802	6.607	623	97.6	32.5	73.67±0.20
1,250	2.7757	0.41838	6.634	35.0	96.7	7.2	73.97±0.31
Total gas			6.593				73.52±0.35
WC70–6: biotite, Adel Mountain Volcanics dike, 56.5 mg; $^{40}Ar/^{36}Ar_a$ = 298.9; *J* value = 0.006338±0.25% (1σ)							
600	0.27470	0.11136	2.287	29.5	37.9	1.9	25.96±0.31
700	0.99913	0.17252	5.791	32.6	64.7	2.9	65.03±0.18
800	3.7713	0.57267	6.585	146	93.9	9.7	73.76±0.20
850	2.5019	0.37570	6.659	157	96.4	6.4	74.57±0.21
900	3.2742	0.49129	6.665	157	96.3	8.4	74.64±0.28
950	7.0107	1.0436	6.718	162	97.1	17.8	75.22±0.20
1,000	7.7855	1.1677	6.668	145	97.7	19.9	74.67±0.20
1,050	7.6052	1.1438	6.649	84.0	98.3	19.5	74.46±0.20
1,150	4.8610	0.73257	6.636	10.3	98.5	12.5	74.32±0.20
1,300	0.43419	0.06448	6.734	3.99	93.4	1.1	75.40±0.89
Total gas			6.552				73.40±0.21
88AV01(B8578): biotite, Adel Mountain Volcanics dike, 56.2 mg; $^{40}Ar/^{36}Ar_a$ = 298.9; *J* value = 0.006197±0.25% (1σ)							
600	0.55534	0.96553	0.575	16.1	35.0	4.7	6.42±0.05
700	0.90814	0.28299	3.209	12.0	48.2	1.4	35.52±0.22
800	7.7170	1.1821	6.258	51.0	85.1	5.7	68.64±0.19
850	14.507	2.0476	7.085	99.7	97.6	9.9	77.52±0.21
900	18.612	2.6193	7.106	120	98.4	12.6	77.24±0.21
950	21.612	2.9987	7.207	87.2	98.9	14.5	78.82±0.21
1,000	21.152	2.8641	7.385	44.1	98.9	13.8	80.73±0.22

Table A2. $^{40}Ar/^{39}Ar$ incremental heating data for samples of Adel Mountain Volcanics and spatially associated volcanic and intrusive rocks, north-central Montana—*Continued*.

Temp (°C)	$^{40}Ar_R$	$^{39}Ar_K$	$^{40}Ar_R/^{39}Ar_K$	$^{39}Ar/^{37}Ar$	$^{40}Ar_R$ (%)	^{39}Ar (%)	Apparent age (Ma±1σ)
88AV01(B8578): biotite, Adel Mountain Volcanics dike, 56.2 mg; $^{40}Ar/^{36}Ar_a$ = 298.9; *J* value = 0.006197±0.25% (1σ)—*Continued*							
1,025	12.322	1.7359	7.098	39.2	98.2	8.4	77.66±0.21
1,050	21.099	3.0365	6.949	47.7	99.1	14.6	76.06±0.21
1,100	19.078	2.7884	6.842	17.4	99.3	13.4	74.91±0.20
1,150	1.3788	0.20169	6.836	0.96	97.2	1.0	74.85±0.22
1,300	0.10867	0.01661	6.544	0.16	64.5	0.1	71.71±1.49
Total gas			6.705				73.44±0.21
WC91–23: biotite, Shaw Butte intrusion; 50.0 mg; $^{40}Ar/^{36}Ar_a$ = 298.9; *J* value = 0.007283±0.25% (1σ)							
800	0.00471	0.00356	1.322	870	7.6	0.1	17.29±12.14
900	0.15571	0.03261	4.775	4048	75.1	1.2	61.67±2.11
1,000	0.70567	0.12141	5.812	---	82.3	4.6	74.79±0.56
1,050	0.97534	0.16883	5.777	---	97.3	6.4	74.35±0.20
1,100	1.3024	0.22621	5.758	---	97.3	8.5	74.11±0.20
1,150	1.5885	0.27440	5.789	---	98.6	10.2	74.50±0.22
1,200	1.8929	0.33021	5.733	160	98.1	12.4	73.79±0.20
1,250	2.4217	0.42212	5.737	173	98.6	15.9	73.84±0.20
1,300	2.0482	0.35892	5.706	165	97.4	13.5	73.45± 0.22
1,350	2.4461	0.42776	5.718	---	96.6	16.1	73.60±0.20
1,450	1.6561	0.28662	5.778	74.0	95.8	10.8	74.36±0.22
Total gas			5.729				73.74±0.28
WC69–5 hornblende, Adel Mountain intrusion, 260.7 mg; $^{40}Ar/^{36}Ar_a$ = 298.9; *J* value = 0.006351±0.25% (1σ)							
600	0.06314	0.01091	5.789	0.23	5.9	0.1	65.14±4.28
700	0.05834	0.01446	4.034	0.23	2.8	0.1	45.64±1.88
750	0.11139	0.01539	7.240	0.34	18.4	0.1	81.10±0.92
800	0.19750	0.02647	7.461	0.46	21.0	0.1	83.52±0.42
850	0.16962	0.02121	7.996	0.57	8.8	0.1	89.36±1.49
900	0.42566	0.04566	9.322	0.55	3.9	0.2	103.76±4.83
950	1.2955	0.18163	7.133	0.31	14.5	1.0	79.93±0.30
975	2.1016	0.30089	6.985	0.31	31.8	1.6	78.30±0.21
1,000	2.9113	0.41897	6.949	0.30	51.5	2.2	77.91±0.21
1,025	11.181	1.6515	6.770	0.30	73.2	8.9	75.94±0.21
1,050	26.094	3.8163	6.838	0.30	78.4	20.5	76.69±0.21
1,075	33.530	4.6090	7.275	0.30	80.0	24.7	81.48±0.22
1,100	18.673	2.4058	7.762	0.30	89.2	12.9	86.81±0.23
1,150	24.926	3.2279	7.722	0.29	95.3	17.3	86.37±0.23
1,200	5.7262	0.8148	7.028	0.29	89.1	4.4	78.78±0.21
1,250	1.8073	0.24215	7.463	0.30	44.2	1.3	83.54±0.53
1,400	5.8660	0.82934	7.073	0.31	92.6	4.5	79.27±0.21
Total gas			7.253				81.24±0.46
WC70–3: biotite, quartz monzonite sill cut by thrust fault, 66.5 mg; $^{40}Ar/^{36}Ar_a$ = 298.9; *J* value = 0.006338±0.25% (1σ)							
600	0.07426	0.06092	1.219	18.2	16.8	0.8	13.88±0.52
700	0.44885	0.14117	3.179	17.4	35.7	2.0	35.99±0.16
800	2.6179	0.51444	5.089	109	78.6	7.1	57.27±0.19
850	3.1630	0.62201	5.085	187	94.4	8.6	57.22±0.16
900	3.2152	0.62803	5.120	185	96.1	8.7	57.61±0.17
950	4.2248	0.81922	5.157	130	94.9	11.3	58.02±0.16
1,000	5.6398	1.0873	5.187	134	96.2	15.0	58.35±0.16
1,050	6.2633	1.2262	5.108	113	97.5	16.9	57.48±0.16
1,100	5.9510	1.1719	5.078	96.0	97.9	16.2	57.15±0.16

Table A2. $^{40}Ar/^{39}Ar$ incremental heating data for samples of Adel Mountain Volcanics and spatially associated volcanic and intrusive rocks, north-central Montana—*Continued.*

Temp (°C)	$^{40}Ar_R$	$^{39}Ar_K$	$^{40}Ar_R/^{39}Ar_K$	$^{39}Ar/^{37}Ar$	$^{40}Ar_R$ (%)	^{39}Ar (%)	Apparent age (Ma±1σ)
WC70–3: biotite, quartz monzonite sill cut by thrust fault, 66.5 mg; $^{40}Ar/^{36}Ar_a$ = 298.9; *J* value = 0.006338±0.25% (1σ)—*Continued*							
1,150	4.0032	0.79149	5.058	32.6	97.7	10.9	56.92±0.15
1,300	0.88488	0.17413	5.082	11.2	96.2	2.4	57.19±0.19
Total gas			5.042				56.75±0.17
WC91–11: biotite, quartz monzonite sill cut by thrust fault, 68.7 mg; $^{40}Ar/^{36}Ar_a$ = 298.9; *J* value = 0.007079±0.1% (1σ)							
800	0.05692	0.07105	0.801	10.5	9.7	0.7	10.20±0.31
900	0.05808	0.10563	0.550	24.1	27.7	1.1	7.01±0.39
1,000	0.12295	0.05480	2.244	10.5	40.7	0.6	28.43±0.31
1,050	0.95992	0.21282	4.510	52.9	58.6	2.2	56.69±0.09
1,100	2.5560	0.56559	4.519	134	76.3	6.0	56.81±0.10
1,150	3.0886	0.67903	4.549	202	93.2	7.2	57.18±0.09
1,200	2.7697	0.60746	4.559	207	94.7	6.4	57.30±0.09
1,250	2.6923	0.58664	4.589	164	94.5	6.2	57.67±0.09
1,300	4.2681	0.91724	4.653	122	94.2	9.7	58.46±0.09
1,350	6.5609	1.4222	4.613	136	96.5	15.0	57.97±0.09
1,400	6.5129	1.4433	4.512	94.6	96.8	15.2	56.72±0.10
1,450	7.0751	1.5674	4.514	67.2	96.6	16.5	56.74±0.09
1,500	4.6639	1.0320	4.519	31.7	96.1	10.9	56.81±0.09
1,550	0.95269	0.20842	4.571	13.7	90.0	2.2	57.45±0.12
Total gas			4.469				56.19±0.13
WC70–4: hornblende, quartz monzonite sill cut by thrust fault,256.5 mg; $^{40}Ar/^{36}Ar_a$ = 298.9; *J* value = 0.006373±0.25% (1σ)							
800	0.63909	0.02001	31.94	0.84	47.7	0.7	334.2±5.5
900	0.09872	0.01138	8.672	0.35	50.1	0.4	97.04±4.92
1,000	0.35124	0.06431	5.462	0.17	70.8	2.2	61.73±0.39
1,050	2.4705	0.49969	4.944	0.22	89.3	17.2	55.96±0.16
1,075	5.1646	0.99806	5.175	0.22	91.7	34.4	58.54±0.18
1,100	2.3904	0.44556	5.365	0.22	96.1	15.3	60.65±0.16
1,150	2.3555	0.44950	5.240	0.21	95.1	15.5	59.26±0.16
1,200	0.81878	0.15918	5.144	0.21	94.9	5.5	58.19±0.22
1,400	1.3171	0.25701	5.125	0.22	94.6	8.8	57.98±0.16
Total gas			5.373				60.74±0.19
WC70-4: biotite, quartz monzonite sill cut by thrust fault, 55.1 mg; $^{40}Ar/^{36}Ar_a$ = 298.9; *J* value = 0.006267±0.25% (1σ)							
600	0.01902	0.01814	1.048	0.66	4.1	0.5	11.81±2.81
700	0.31295	0.35678	0.877	3.76	10.6	10.2	9.89±0.14
800	1.6703	0.41447	4.030	4.36	44.4	11.8	45.00±0.12
850	1.6187	0.32268	5.016	15.04	68.7	9.2	55.84±0.16
900	1.7111	0.32622	5.245	16.81	75.6	9.3	58.34±0.31
950	2.1074	0.39813	5.293	15.28	70.5	11.3	58.87±0.18
1,000	3.3226	0.59883	5.548	15.36	68.4	17.1	61.66±0.25
1,025	2.3676	0.44330	5.341	15.81	78.9	12.6	59.39±0.18
1,050	1.4434	0.27414	5.265	6.30	82.1	7.8	58.56±0.20
1,100	1.1726	0.22633	5.181	3.45	84.6	6.5	57.64±0.27
1,150	0.54993	0.10627	5.175	1.19	84.4	3.0	57.58±0.48
1,300	0.11960	0.02280	5.245	0.20	74.7	0.7	58.34±2.62
Total gas			4.679				52.14±0.31
WC70–5: hornblende, monzonite dike that cuts thrust fault, 294.3 mg; $^{40}Ar/^{36}Ar_a$ = 298.9; *J* value = 0.006318±0.25% (1σ)							
800	0.16464	0.03564	4.619	1.17	25.4	1.5	51.89±1.52

Table A2. $^{40}Ar/^{39}Ar$ incremental heating data for samples of Adel Mountain Volcanics and spatially associated volcanic and intrusive rocks, north-central Montana—*Continued.*

Temp (°C)	$^{40}Ar_R$	$^{39}Ar_K$	$^{40}Ar_R/^{39}Ar_K$	$^{39}Ar/^{37}Ar$	$^{40}Ar_R$ (%)	^{39}Ar (%)	Apparent age (Ma±1σ)
WC70–5: hornblende, monzonite dike that cuts thrust fault, 294.3 mg; $^{40}Ar/^{36}Ar_a$ = 298.9; *J* value = 0.006318±0.25% (1σ)—*Continued*							
900	0.05523	0.01166	4.738	0.57	51.3	0.5	53.21±3.30
1,000	0.20139	0.04806	4.190	0.13	74.3	2.0	47.14±0.64
1,025	0.45478	0.10816	4.205	0.14	90.1	4.6	47.30±0.28
1,050	0.95254	0.22628	4.210	0.15	92.7	9.5	47.36±0.13
1,075	1.0423	0.24695	4.221	0.15	93.4	10.4	47.48±0.20
1,100	1.7675	0.41946	4.214	0.15	95.1	17.7	47.40±0.14
1,150	3.9976	0.94505	4.230	0.15	96.7	39.8	47.58±0.13
1,200	1.0890	0.25795	4.222	0.15	93.8	10.9	47.49±0.15
1,400	0.35366	0.07559	4.678	0.18	81.0	3.2	52.55±0.46
Total gas			4.244				47.73±0.18
WC69–2: hornblende, monzonite dike that cuts thrust fault, 95.0 mg; $^{40}Ar/^{36}Ar_a$ = 298.9; *J* value = 0.006338±0.25% (1σ)							
800	0.02755	0.00746	5.787	0.50	8.3	0.5	64.98±21.1
900	0.04379	0.00823	5.321	0.41	32.3	0.9	59.84±3.86
1,250	0.06250	0.01259	4.966	0.15	61.8	1.4	55.90±1.66
1,050	0.39326	0.09464	4.155	0.17	91.0	10.8	46.89±0.59
1,100	0.92804	0.21995	4.219	0.16	95.2	25.1	47.61±0.23
1,150	1.3264	0.31504	4.210	0.16	96.1	36.0	47.51±0.25
1,250	0.91075	0.22001	4.140	0.15	95.0	25.1	46.73±0.18
Total gas			4.219				47.61±0.38

indicates that the monzonite may postdate thrust deformation (see discussion in text). Location: NE¼SE¼NE¼ sec. 11, T. 16 N., R. 6 W., Johnson Mountain 7.5-minute USGS quadrangle, Lewis and Clark County, Montana. Latitude and longitude: 47.1593°N., 112.3158°W.

WC70-3. Biotite. Biotite-bearing monzonite porphyry sill intruding the lower part of the sedimentary member of the western facies of the Upper Cretaceous Two Medicine Formation. Exposed in road cut on Deadman Coulee Road. Map unit TKp of Schmidt (1972c). Location: NW¼SW¼ sec. 8, T. 16 N., R. 4 W., Comb Rock 7.5-minute USGS quadrangle, Lewis and Clark County, Montana. Latitude and longitude: 47.1572°N., 112.1467°W.

WC91-11. Biotite. Biotite-bearing monzonite porphyry sill intruding the lower part of the sedimentary member of the western facies of the Upper Cretaceous Two Medicine Formation. Exposed in fresh road cut on north side of Deadman Coulee Road. Map unit TKp of Schmidt (1972c). The sample locality is likely the same or similar exposure from which sample WC70-3 was collected by R.G. Schmidt and H.H. Mehnert in 1970. Location: Comb Rock 7.5-minute USGS quadrangle, Lewis and Clark County, Montana. Latitude and longitude: 47.1573°N., 112.1463°W.

WC70-4. Hornblende and biotite. Biotite-bearing quartz monzonite porphyry sill. Sill intrudes the Upper Cretaceous Telegraph Creek Formation, Virgelle Sandstone, and lower part of the western facies of the Two Medicine Formation. Sill is exposed in the upper part of a steep ravine on the east side of a prominent ridge ("The Reef") about 2.7 km north of Deadman Coulee Road. Location: NE¼SW¼ sec. 31, T. 17 N., R. 4 W, Comb Rock 7.5-minute USGS quadrangle, Lewis and Clark County, Montana. Approximate latitude and longitude: 47.1806°N., 112.1625°W.

WC70-5. Hornblende. Hornblende monzonite dike. Dike intrudes volcanic member of western facies of Two Medicine Formation. Dike is exposed in road cut on secondary Highway 434 through Rattlesnake Reef. Location: NW¼NE¼NW¼ sec. 8, T. 15 N., R. 4 W., Roberts Mountain 7.5-minute USGS quadrangle, Lewis and Clark County, Montana: Approximate latitude and longitude: 47.0778°N., 112.1417°W.

WC69-2. Hornblende. Hornblende monzonite dike. Rock is fine grained and composed of small crystals of sanidine, oligoclase, hornblende, augite, green biotite, quartz, apatite and magnetite. The sample is from a 0.4- to 3.1-m-thick vertical dike that intrudes clastic rocks of the volcanic member of the Upper Cretaceous Two Medicine Formation. From the sampling locality, the dike extends northwest, crosses the trace of the Eldorado thrust, and extends into Middle Proterozoic strata of the Belt Supergroup in the hanging wall of the Eldorado thrust plate. Dike is exposed in road cut on east side of Stearns Wolf Creek Road. Location: NE¼NE¼NE¼ sec. 29, T. 15 N., R. 4 W., Roberts Mountain 7.5-minute USGS quadrangle, Lewis and Clark County, Montana: Approximate latitude and longitude: 47.0778°N., 112.1417°W.